AFCRL-70-0373 U-4829

INVESTIGATION OF THE ABSORPTION OF INFRARED RADIATION BY ATMOSPHERIC GASES

Darrell E. Burch
David A. Gryvnak
John D. Pembrook

Philco-Ford Corporation
Aeronutronic Division
Ford Road
Newport Beach, California 92663

Contract No. F19628-69-C-0263
Project No. 5130

Semi-Annual Technical Report No. 1

June 1970
This research was supported by the Advanced Research Projects Agency under ARPA Order No. 1366.

Contract Monitor: Robert A. McClatchey
Optical Physics Laboratory

Prepared for
AIR FORCE CAMBRIDGE RESEARCH LABORATORIES
UNITED STATES AIR FORCE
BEDFORD, MASSACHUSETTS 01730

Qualified requestors may obtain additional copies from the Defense Documentation Center. All others should apply to the Clearinghouse for Frederal Scientific and Technical Information.

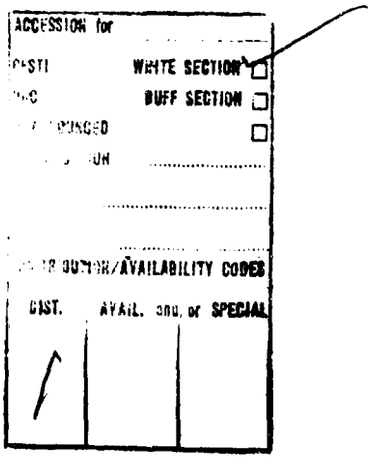

AFCRL-70-0373 U-4829

INVESTIGATION OF THE ABSORPTION OF INFRARED RADIATION BY ATMOSPHERIC GASES

Darrell E. Burch
David A. Gryvnak
John D. Pembrook

Philco-Ford Corporation
Aeronutronic Division
Ford Road
Newport Beach, California 92663

Contract No. F19628-69-C-0263
Project No. 5130

Semi-Annual Technical Report No. 1

June 1970
This research was supported by the Advanced Research Projects Agency under ARPA Order No. 1366.

Contract Monitor: Robert A. McClatchey
Optical Physics Laboratory

Prepared for
AIR FORCE CAMBRIDGE RESEARCH LABORATORIES
UNITED STATES AIR FORCE
BEDFORD, MASSACHUSETTS 01730

ABSTRACT

From spectral transmittance curves of very large samples of CO_2 we have determined coefficients for intrinsic absorption and pressure-induced absorption from approximately 1130 cm^{-1} to 1835 cm^{-1}. Most of the pressure-induced absorption arises from the forbidden ν_1 and $2\nu_2$ bands of the $O^{16}C^{12}O^{16}$ molecule, and the major portion of the intrinsic absorption arises from the same bands of the $O^{16}C^{12}O^{18}$ molecule. Curves of the absorption coefficients for samples of CO_2 pressurized to approximately 10 atm, or more, with He are presented throughout most of the region from 1885 cm^{-1} to 2132 cm^{-1}. These curves and a table of the integrated absorption coefficient are adequate to determine the strengths of most of the bands of significance in this region. Spectral transmittance curves of CO_2 absorption between approximately 2065 cm^{-1} and 2100 cm^{-1} are presented for a variety of samples. Curves of the pressure-induced absorption by N_2 are presented for the 2400-2650 cm^{-1} region.

TABLE OF CONTENTS

TABLE OF CONTENTS (Cont.)

TABLE OF CONTENTS (Cont.)

SECTION 1

SUMMARY AND DEFINITION OF TERMS

The absorption in atmospheric windows frequently cannot be treated by band-model methods which are applicable to spectral regions containing strong absorption bands. A significant portion of the attenuation in windows may result from continuum absorption due to the extreme wings of distant lines or to pressure-induced bands. The functional dependence of the continuum absorption on such parameters as path length, temperature, pressure, and atmospheric composition is quite different from that of line absorption. Laboratory studies of atmospheric gases under controlled conditions frequently are required to determine the portion of the absorption due to the continuum.

This report deals with a variety of situations in which continuum absorption and weak-line absorption are important. Section 2 deals with continuum absorption between approximately 2400 and 2650 cm^{-1} due to a pressure-induced band of N_2 and to the extreme wings of CO_2 lines centered at lower wavenumbers. Pressure-induced bands and weak forbidden bands of CO_2 in the 1100-2000 cm^{-1} region are discussed in Section 3. By studying samples covering a wide range of pressures and path lengths, we have determined the contribution due to the continuum produced by the pressure-induced bands and that due to the weak bands which contain rotational line structure. We have been able to measure the CO_2 absorption, even in the regions of very weak absorption near 1830 cm^{-1} and 1130 cm^{-1}.

Several CO_2 bands which occur between 1890 and 2130 cm^{-1} play a significant role in the absorption by long atmospheric paths. Section 4 includes experimental curves and tables from which the strengths of several of these bands can be determined. Also included in Section 4 are transmittance curves and tabulated results for several samples studied near 2080 cm^{-1}.

A prominent feature in the spectrum near this wavenumber has proven to be useful in analyzing spectral curves obtained by aircraft. Section 5 contains a summary of experimental data which we have obtained previously and have recently put on magnetic tape. The tapes and a user's manual will be available in the near future for workers who need them.

All of the data included in this report are based on samples contained in one of two multiple-pass absorption cells which have been described previously.[1] The base lengths of the cells are approximately 29 m and 1 meter. Sample pressures up to 2.5 atmospheres are employed in the long cell; 21 atm is the maximum pressure used in the short cell.

The absorber thickness, u, of a gas sample is given by

$$u(\text{molecules/cm}^2) = 2.69 \times 10^{19}\ p^*(\text{atm})\ L(\text{cm})\ (273/\theta)$$
$$= 7.34 \times 10^{21}\ p^*\ L/\theta. \qquad (1\text{-}1)$$

The temperature θ is in degrees Kelvin, and L is the geometrical path length through the sample. The density-equivalent-pressure p* of the absorbing gas approaches its pressure p at low pressures. Because of the non-linear relationship between the density and the pressure of a gas, p* may differ significantly from p at high pressures. For the gases and pressures used in the present investigation, the following expression is sufficiently accurate.

$$p^* \quad p(1 + c\ p) \qquad (1\text{-}2)$$

The pressures are in atm and, near room temperature, c = 0.005 for N_2O and CO_2, and 0.001 for N_2 and O_2. For the largest sample of CO_2, p* is only approximately 11% greater than p; in many of the samples the difference is negligible. In the following discussion certain quantities are said to be proportional to pressure; it should be borne in mind that the more correct quantity, density-equivalent pressure p*, was used in the calculations where the difference between p* and p was significant.

The true transmittance that would be observed with infinite resolving power is given by

$$T' \quad \exp(-u\kappa), \qquad \text{or} \qquad (-1/u)\,\mathcal{L}\,T' = \kappa, \qquad (1\text{-}3)$$

where κ is the absorption coefficient. Because of possible variations in κ with wavenumber and the finite slitwidth of a spectrometer, the observed transmittance T may differ from T' at the same wavenumber. The quantity T represents a weighted average of T' over the interval passed by the spectrometer.

Throughout this report we deal with three different basic types of absorption. In some spectral regions, an appreciable portion of the absorption is due to the extreme wings of lines whose centers are several cm^{-1} away. This wing absorption has the nature of a continuum, i.e., there is no structure, and because of the collision broadening of the lines, the absorption coefficient C_w due to the wing absorption is proportional to pressure. ($C_w = C_w^o p^*$) (See Eq. 1-6 and the discussion following it.)

Anotner type of continuum absorption arises from pressure-induced bands; the absorption coefficient, C_p, for pressure-induced absorption is also proportional to pressure. The absorption coefficient due to local lines whose centers occur within a few cm^{-1} of the point of observation is denoted by κ(local). The latter quantity may vary rapidly with wavenumber and depends on pressure because of collision-broadening of the absorption lines.

At a given wavenumber, there may be appreciable absorption due to local lines, the wing continuum, the pressure-induced continuum, or to any of these three. Therefore, the total absorption coefficient κ in Eq. (1-3) may be given by

$$\kappa = \kappa(\text{local}) + C_w + C_p. \qquad (1\text{-}4)$$

For a sample of absorbing gas only, such as several of the CO_2 samples discussed below, we can rewrite Eq. (1-4) as

$$\kappa = \kappa(\text{local}) \quad (C^o_{s,w} + C^o_{s,p})\, p^*, \quad \text{(absorbing gas only)} \qquad (1\text{-}4a)$$

where the normalized coefficients $C^o_{s,w}$ and $C^o_{s,p}$ are the values of C_w and C_p, respectively, when $p^* = 1$. The subscript s denotes self-broadening of the lines or self-induced absorption. Since u is proportional to pL, ($-\Delta T$) due to wing continuum or pressure-induced continuum is proportional to p^2L.

We frequently are concerned with samples containing a non-absorbing gas, along with the absorbing gas. This gas broadens the absorption lines and may induce additional absorption by the pressure-induced bands of the absorbing gas. For a mixture of an absorbing gas and a broadening gas,

Eq. (1-4) becomes

$$\kappa = \kappa(\text{local}) + (C^{o}_{s,w} + C^{o}_{s,p})\, p^{*} + (C^{o}_{b,w} + C^{o}_{b,p})\, p_{b}^{*}. \qquad (1\text{-}4b)$$

$C^{o}_{b,w}$ and $C^{o}_{b,p}$ are the normalized coefficients for wing absorption and pressure-induced absorption by the absorbing gas due to the presence of the broadening gas denoted by subscript b.

The intrinsic absorption coefficient due to a single collision-broadened absorption line at a point within a few cm^{-1} of the line center, ν_o, is given by the Lorentz shape:

$$k = \frac{S}{\pi} \frac{\alpha}{(\nu-\nu_o)^2 + \alpha^2}. \qquad (1\text{-}5)$$

The line strength $S = \int k d\nu$ is essentially independent of pressure for the conditions of the present study. It has been shown[2,3] that for $|\nu-\nu_o|$ greater than a few cm^{-1}, the Lorentz equation may require modification by a factor of χ, which is a function of $(\nu-\nu_o)$. Therefore, Eq. (1-5) becomes

$$k = k_L \chi = \frac{S}{\pi} \frac{\alpha \chi}{(\nu-\nu_o)^2 + \alpha^2} \qquad (1\text{-}6)$$

where k_L denotes the value given by the Lorentz equation. The value of χ is approximately equal to unity for small $|\nu-\nu_o|$, but may be as small as 0.01 for CO_2 lines when $(\nu-\nu_o)$ is as large as 100 cm^{-1}.

The half-width α is proportional to pressure so that k is, in turn, proportional to pressure in the extreme wings where $|\nu-\nu_o| \gg \alpha$. Thus, the continuum absorption coefficient due to the extreme wings of many lines is proportional to pressure, as stated above.

SECTION 2

ATMOSPHERIC ABSORPTION BY N_2 BETWEEN 2400 AND 2600 cm^{-1}

The fundamental vibration band of N_2 is centered near 2330 cm^{-1} and produces measurable absorption from less than 2200 cm^{-1} to more than 2600 cm^{-1}. We have investigated the absorption by this band between approximately 2390 cm^{-1} and 2650 cm^{-1} because of its important role in atmospheric transmission in this region. Below 2390 cm^{-1} the CO_2 absorption in the atmosphere is much greater than the N_2 absorption. The N_2 band is pressure induced so that the probability of a transition in a given molecule is proportional to pressure, and the absorptance by a short path is proportional to p^2.

Shapiro and Gush[4] have published spectral data on N_2 absorption for samples at approximately 20 atm pressure. Farmer et al[5] have also measured the absorption between 2400 cm^{-1} and 2525 cm^{-1} by approximately 1 atm of pure N_2 with path lengths of a few hundred meters. The results of Farmer et al are consistent with the high-pressure data of Shapiro and Gush if $(-\ln T)$ is assumed to be proportional to p^2L, according to the discussion following Eq. (1-4a). The work reported here was undertaken to check the previous work and to determine the appropriate coefficient $C^o_{0,p}$ for N_2 absorption induced by O_2. From the value of this coefficient and the corresponding coefficient, $C^o_{s,p}$, for self-induced absorption by N_2, we have calculated the transmittance by N_2 in the earth's atmosphere from approximately 2390 cm^{-1} to 2650 cm^{-1}.

Values of the absorber thickness of N_2 were calculated by use of Eqs. (1-1) and (1-2). Since there is no absorption by N_2 other than that which is pressure induced, Eqs. (1-3) and (1-4a) combine to give

$$-\frac{1}{u}\ln T = p^* C^o_{s,p} \qquad (2\text{-}1)$$

for a pure N_2 sample, and

$$-\frac{1}{u}\ln T = p^* C^o_{s,p} + p^*_{O_2} C^o_{O,p} \qquad (2\text{-}1a)$$

for a sample of $N_2 + O_2$. Since the true transmittance T' changes slowly with wavenumber in continuum absorption, the observed transmittance T is essentially equal to T'. Note that $C^o_{O,p}$ corresponds to absorption by N_2 that is induced by O_2; the O_2 does not absorb. We detected no absorption by a sample of 8 atm of O_2 with a 32.9 meter path length. After values of $C^o_{s,p}$ had been found from pure N_2 samples, we determined $C^o_{O,p}$ from data on $O_2 + N_2$ mixtures by use of Eq. (2-1a). The results for pure N_2 and for $O_2 + N_2$ mixtures are summarized in Fig. (2-1). The good agreement among the pure N_2 data at different pressures provides evidence of the pressure dependence assumed in deriving Eq. (2-1). Below approximately 2500 cm^{-1}, our results for pure N_2 differ by less than $\pm$ 5% from those by Shapiro and Gush.[4] At larger wavenumbers, the agreement is within the accuracy to which the curves of Shapiro and Gush can be read. Data obtained from samples of N_2 with 5 atm of O_2 compared well with data from samples of N_2 with 8 atm of O_2, indicating the validity of the term involving p^*_b in Eq. (2-1a).

Air contains approximately 78 percent N_2, 21 percent O_2, and 1 percent other gases. Therefore, at 296°K and 1 atm pressure, there are $0.78 \times 2.48 \times 10^{24} = 1.93 \times 10^{24}$ molecules of N_2/cm^2 in a 1 kilometer path. From Fig. (2-1) we see that $C^o_{O,p} \approx 0.95\ C^o_{s,p}$; therefore, the "effective" pressure of 1 atm air is approximately 0.99 atm. It follows that $(-\ln T)$ for a 1 km air path at 1 atm is $0.99 \times 1.93 \times 10^{24}\ C^o_{s,p}$. We have used this relationship along with the curve of $C^o_{s,p}$ from Fig. (2-1) to calculate $(-\ln T)$ versus wavenumber for 1 km of air. The results are plotted in Fig. (2-2).

Also shown for comparison in Fig. (2-2) is a curve corresponding to the continuum due to the extreme wings of the very strong CO_2 lines centered between approximately 2250 cm^{-1} and 2390 cm^{-1}. This curve is based on data obtained in our laboratory and reported previously.[2,6]

Near 2400 cm^{-1}, N_2 and CO_2 are seen to absorb approximately the same, but above 2420 cm^{-1} the N_2 absorption is much greater. The upper curve represents both the N_2 absorption and the CO_2 wing absorption. The quantity $(-\ln T)$ can be calculated for other pressures by making use of the knowledge that it is proportional to the square of the total pressure P. Some additional CO_2 absorption not accounted for in Fig. (2-2) occurs because

of weak bands of the $C^{12}O^{16}O^{18}$ and $C^{12}O^{16}O^{17}$ isotopes and a pressure-induced band of the common isotope $C^{12}O_2^{16}$. (See Reference 6.) N_2O and H_2O also absorb in the spectral region covered in the figure with the strongest absorption by these two gases occurring above 2500 cm^{-1}. Thus, the N_2 absorption plays its most important role between 2400 cm^{-1} and 2500 cm^{-1}.

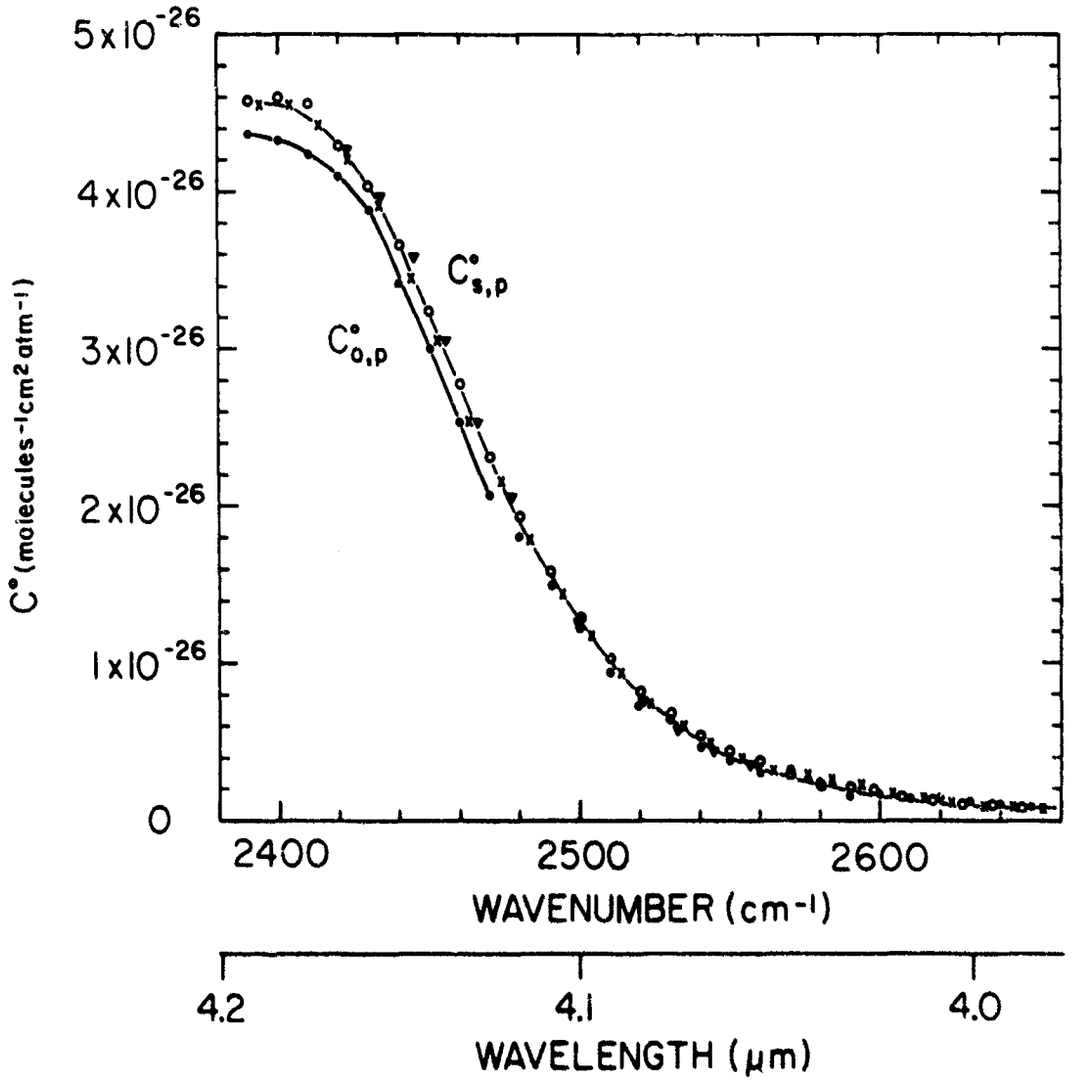

FIG. 2-1. Normalized Coefficients of Pressure-Induced N_2 Absorption Plotted Versus Wavenumber. The upper curve represents $C^{o}_{s,p}$ and is based on pure N_2. The various geometrical figures correspond to the following samples of pure N_2: ▽, L = 36.9 m, p = 14.6 atm; x, L = 32.9 m, p = 13.6 atm; O, L = 32.9 m, p = 21.8 atm. The temperature is 296°K. The lower curve represents $C^{o}_{o,p}$ and is based on mixtures of approximately 14 atm N_2 + 8 atm O_2 with L = 32.9 m.

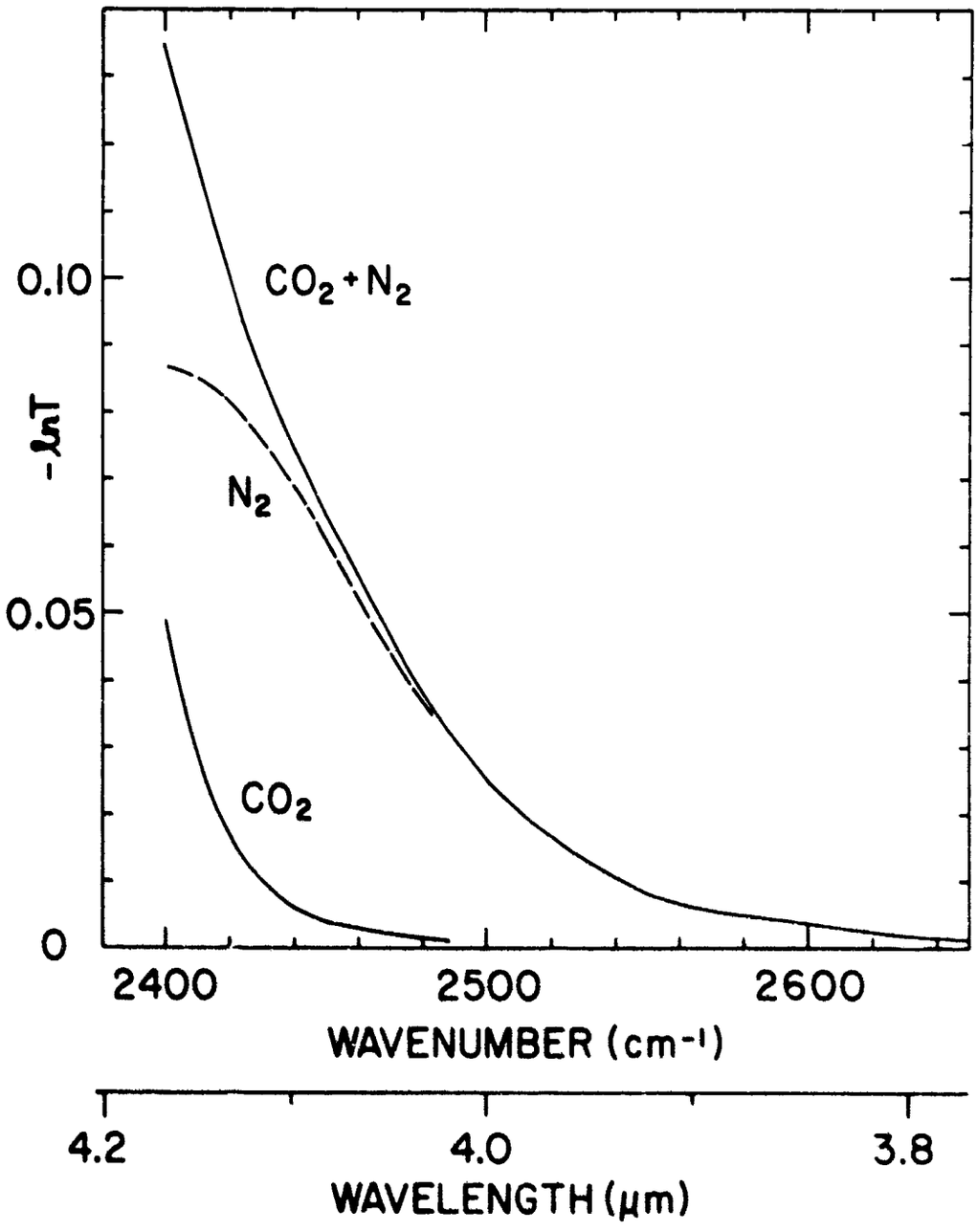

FIG. 2-2. Curves of $-\ln T$ of N_2 and the Continuum Due to the Extreme Wings of CO_2 Lines. The curves correspond to a 1 km path of air at 296°K and 1 atm pressure.

SECTION 3

ABSORPTION BY LARGE SAMPLES OF CO_2 BETWEEN 1100 AND 2000 cm^{-1}

Absorption by CO_2 is relatively weak throughout the 1100 - 2000 cm^{-1} (9.1 - 5 μm) region and has not been studied as thoroughly as most of the remainder of the spectrum. Figures 3-1, 3-2, and 3-3 show spectral transmittance curves for a variety of large samples at room temperature, 296°K. Some of the absorption is due to intrinsic bands, some to pressure-induced bands, and a small amount to wing absorption. From the transmittance maximum near 1130 cm^{-1} to approximately 900 cm^{-1}, most of the absorption is due to the bands involved in the well-known laser transitions. Several medium and strong bands occur between 2000 and 2400 cm^{-1}; some of them are discussed in Section 4. Samples B and C represented in Fig. 3-3 are essentially opaque from 2020 cm^{-1} to beyond 2400 cm^{-1}. Data for the portions of the curves in Fig. 3-3 on either side of approximately 1590 cm^{-1} were obtained at different times with different gratings in the spectrometer.

Most of the absorption between 1130 and 1500 cm^{-1} is due to the ν_1 and $2\nu_2$ bands. The positions of the centers of these bands have been calculated for the four most common isotopes from the energy levels tabulated by Stull, Wyatt, and Plass[7] and are listed in Table 3-1. Also listed are bands which have the same change in quantum numbers but arise from the lowest excited vibrational energy level. New notations for the identification of CO_2 energy levels and isotopes are described as footnotes of Table 3-1; the new notations are used hereafter. The bands listed are forbidden for the symmetric 626 and 636 molecules at low pressures; however, as the pressure increases, the interaction of the molecules with their neighbors disturbs the symmetry so that the transitions may occur. As discussed in Section 1, the absorption coefficient for these pressure-

TABLE 3-1

CENTERS OF CO_2 BANDS BETWEEN 1100 AND 1450 cm^{-1} [a]

Isotope [b]	$(100,0)_I$ [c] $[10^00]$	$(100,0)_{II}$ $[02^00]$	$(110,1)_I$-$(010,1)_I$ $[11^10$-$01^10]$	$(110,1)_{II}$-$(010,1)_I$ $[03^10$-$01^10]$
626	1388.20	1285.43	1409.45	1265.11
636	1370.11	1265.84	1388.65	1248.03
628	1365.89	1259.49	1386.93	1239.29
627	1376.03	1272.35	1397.28	1251.98

[a] Band centers are in cm^{-1} and are based on energy levels tabulated by Stull, Wyatt, and Plass.[7]

[b] The number in the first column refers to the isotopic species. 626 corresponds to $O^{16}C^{12}O^{16}$, 636 to $O^{16}C^{13}O^{16}$, 628 to $O^{16}C^{12}O^{18}$, and 627 to $O^{16}C^{12}O^{17}$.

[c] The lower energy level is the ground state when only one level is given. Two different notations are given for the energy levels involved in the transitions. The notation in brackets is widely used. The other notation has certain advantages and is gaining acceptance. Since $v_1 \cong 2v_2$ for CO_2, the two energy levels 10^00 and 02^00 are approximately the same, as are 10^01 and 02^01, etc. In order to illustrate the relationship between the old and new notations, we consider the three energy levels given in the old notation by 20^03, 12^03, and 04^03. Note that quantum numbers v_3 and ℓ are both fixed and that $2v_1 + v_2$ is constant. In the new notation the three levels become $(203,0)_I$, $(203,0)_{II}$, and $(203,0)_{III}$. The Roman numeral subscript denotes the order in which the bands occur without regard to the assignment of v_1 or v_2; I denotes the highest wavenumber, II the second highest, etc. The first digit in the parenthesis is the largest value of v_1 in a group; the second is the smallest value of v_2. The third digit is v_3 and the one following the comma is ℓ.[2]

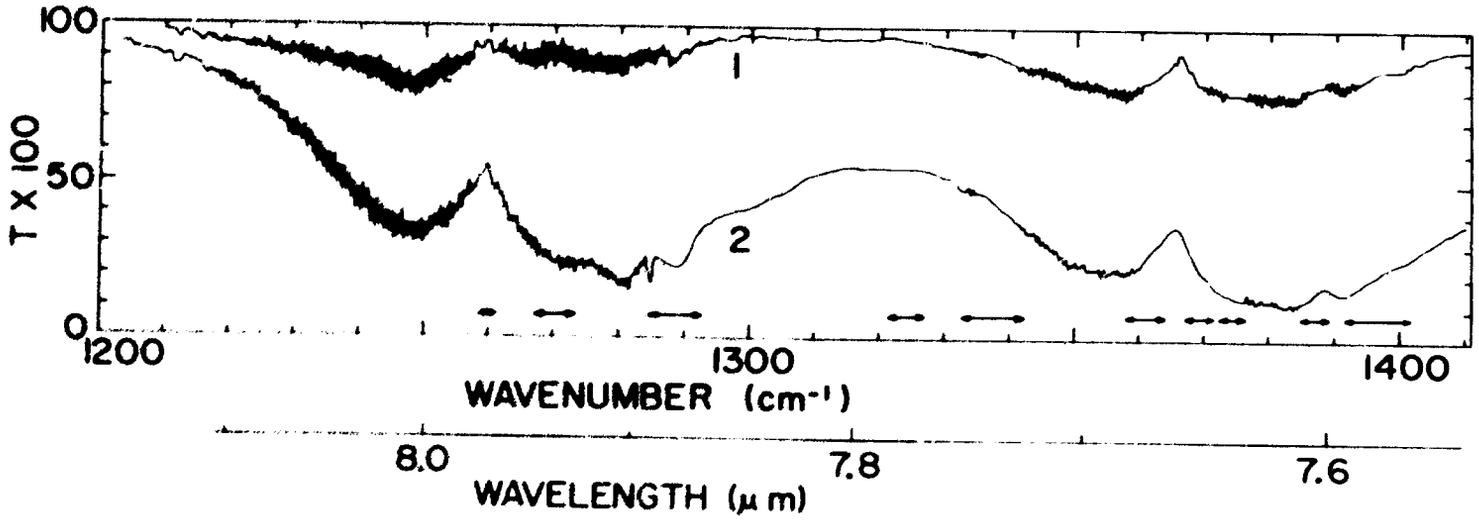

FIG. 3-1. Spectral Transmittance Curves of Two Relatively Low-Pressure Samples of CO_2 Between 1200 and 1400 cm^{-1}. The spectral slitwidth varies from approximately 0.45 cm^{-1} at 1200 cm^{-1} to 0.65 at 1400 cm^{-1}. In some places where the H_2O absorption covered an area which included as many as 5 or 6 CO_2 lines, we made no attempt to reconstruct the CO_2 structure. Instead a smooth line was drawn to represent the average CO_2 transmittance. Intervals containing significant absorption by H_2O are indicated by arrows. The curves in this figure were obtained as part of a previous study[8] in our laboratory. The sample parameters are: Sample 1, p 0.25 atm, L 713 m; Sample 2, p 1.05 atm, L 359 m.

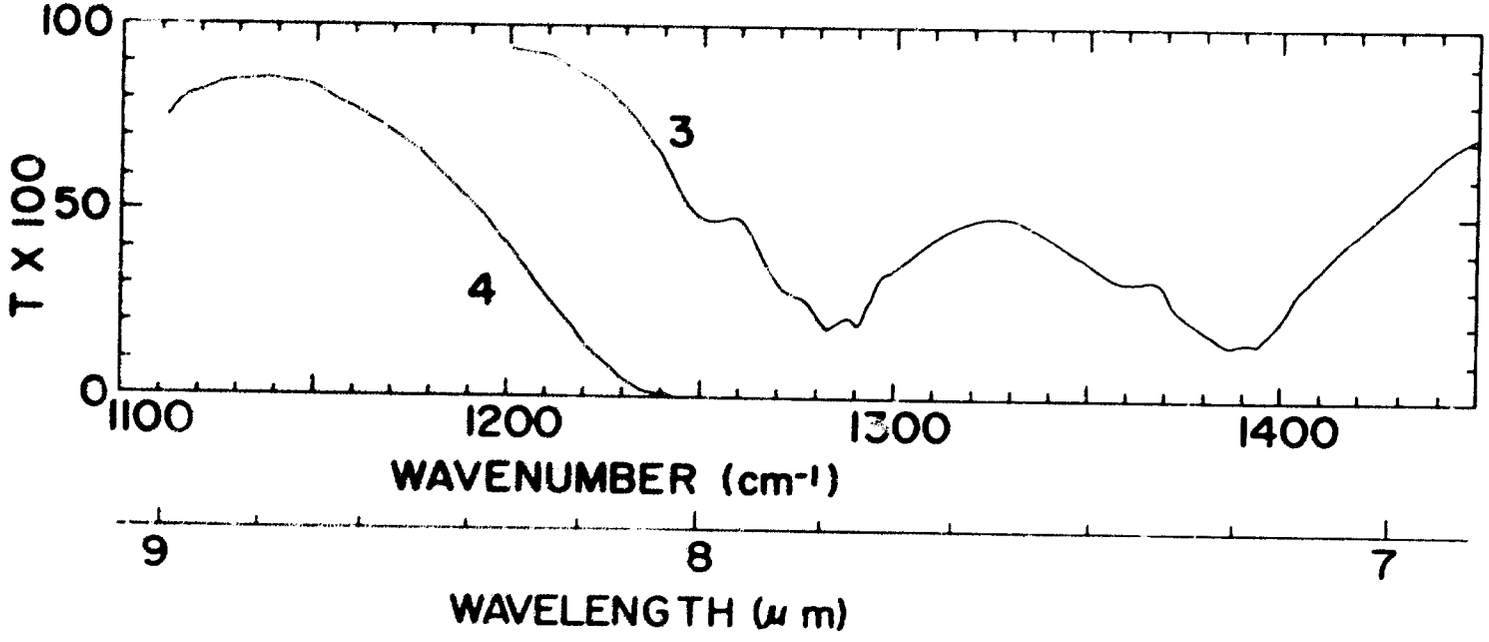

FIG. 3-2. Spectral Transmittance Curves of Two High-Pressure Samples of CO_2 Between 1100 and 1450 cm^{-1}. The spectral slitwidth varies from approximately 2.0 cm^{-1} at 1100 cm^{-1} to 3.6 cm^{-1} at 1450 cm^{-1}. The sample parameters are: Sample 3, p = 3.70 atm, L = 32.9 m; Sample 4, p = 14.6 atm, L = 32.9 m.

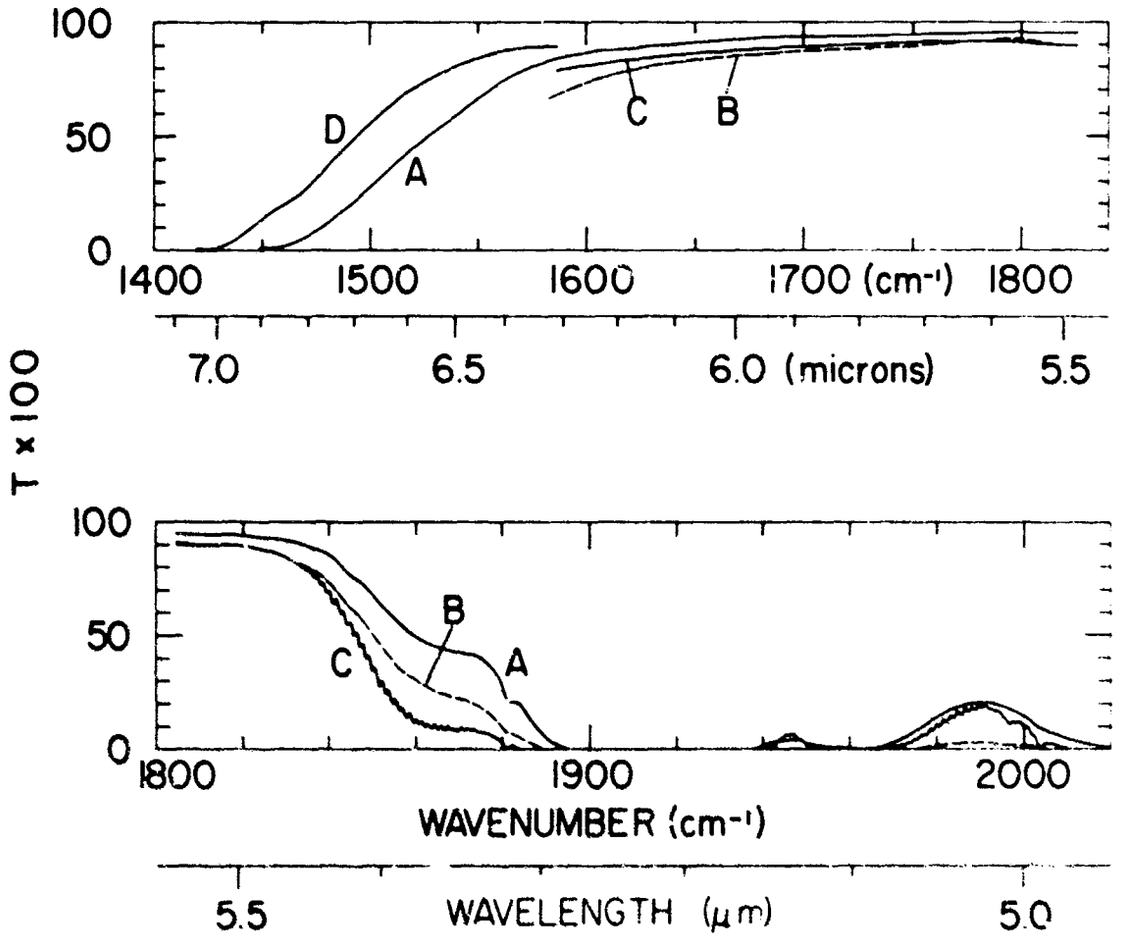

FIG. 3-3. Spectral Transmittance Curves from 1400 cm^{-1} to 2020 cm^{-1}. The spectral slitwidth varies from approximately 0.55 cm^{-1} at 1500 cm^{-1} to 1.0 cm^{-1} at 2000 cm^{-1}. The samples are pure CO_2 and the parameters are:

Sample	p (atm)	L (meters)
A	14.6	32.9
B	21.3	32.9
C	2.35	933
D	1.82	1067

induced bands is proportional to p, and $(-\ell n T)$ is proportional to $p^2 L$. Because of the asymmetry of the 628 and 627 molecules, they can absorb at low pressures, and the dependence of their absorption on pressure and absorber thickness is similar to that of other intrinsic absorption bands. We expect the 628 bands to be approximately 10 times as strong as the corresponding 627 bands since the asymmetry of the former molecule is twice as much and the abundance is 5 times as great as that of the latter. Any absorption by one of these bands of the 636 molecule would be pressure-induced, and the ratio of its strength to that of the corresponding 626 band is probably about 1.1:99, the ratio of the abundances of C^{13} and C^{12}.

The strength of each difference band with $(010,1)_I$ as the lower state is expected to be approximately 4 percent as great as the associated fundamental or overtone band which arises from the same change in quantum numbers. This relationship is based on the assumption that the strengths are proportional to the populations of the lower energy levels. At room temperature the population of the $(010,1)_I$ level is approximately 4% of the (000,0) level.

On the basis of the above discussion, we expect most of the pressure-induced absorption to result from the $(100,0)_I$ and $(100,0)_{II}$ bands of the 626 molecule and the major portion of the intrinsic absorption to arise from the same bands of the 628 molecule. Furthermore, we expect the fraction of the absorption due to the pressure-induced bands to increase with increasing pressure. Figures 3-1 and 3-2 confirm these expectations. Sample 1, which has a relatively low pressure and long path, shows two distinct band centers near 1260 and 1366 cm^{-1}, the calculated positions of the 628 band centers given in Table 3-1. Sample 3, which is at 3.70 atm shows transmittance minima near 1285 and 1388 cm^{-1}, the calculated band centers for the 626 molecule. The 628 bands have been observed with relatively coarse resolution by Eggers and Arends[9] from samples enriched in O^{18}. The positions of the band centers determined by these workers agree with ours to less than the experimental uncertainties. The pressure-induced 626 bands have been observed by Welsh, Crawford, and Locke.[10]

The major errors result from errors in placing the zero-absorptance curves on the sample curves and from absorption by H_2O which appeared as an impurity in the CO_2 in spite of efforts to keep it dry. Much of the H_2O absorption was accounted for before the curves were replotted by comparing the original sample curves with spectral curves of H_2O with N_2 as a broadening gas. Spectral regions between 1100 and 1400 cm^{-1} where H_2O absorption was partially accounted for are indicated by arrows in Fig. 3-1. The H_2O absorption was most serious between 1500 and 1800 cm^{-1} because the H_2O lines are stronger and the CO_2 absorption is weaker. The large amount of gas required for the long cell could not be purified as effectively as the smaller amount required to fill the short cell.

Furthermore, the absorption by H_2O is approximately proportional to the pressure of a mixture of constant composition while the pressure-induced CO_2 absorption is proportional to the square of the pressure. Therefore, the H_2O absorption was less important for the high-pressure samples in the short cell than for the lower-pressure samples in the long cell.

In regions where there is intrinsic absorption due to local lines and pressure-induced absorption, but no wing absorption, Eq. (1-4a) reduces to

$$\kappa = \kappa(\text{local}) + C_{s,p} = \kappa(\text{local}) + C^{o}_{s,p}\, p^{*}.$$

Since $C_{s,p}$ is proportional to p^*, and κ(local) is not, we have been able to determine each of these quantities from spectral curves of two or more samples at quite different pressures. At pressures less than a few atm, κ(local) varies rapidly with wavenumber because of the line structure. Since the spectral slitwidth of the spectrometer was greater than the line widths at low pressures, κ(local), and thus κ, could not be measured directly at a given wavenumber. We were not interested in retaining all of the structure in the spectra, but in the values of the constants averaged over intervals approximately 5-10 cm^{-1} wide. The strength, $S = \int k\,d\nu$, of an intrinsic absorption line is independent of pressure; therefore, the average of κ(local), which may result from several neighboring lines, is essentially independent of pressure if the interval is several line widths wide and contains the centers of all the lines contributing to the absorption.

If we consider only the true transmittance of the local lines, $(-1/u)\overline{\ln T'}(\text{local})$ is equivalent to κ(local). (The bar represents an average over wavenumber, and the prime denotes true transmittance that would be observed with infinite resolving power.) However, we do not read $-\overline{\ln T'}$ from a spectral curve, but a slightly different quantity, $-\ln \bar{T}$, since we average the observed transmittance curve over a 5-10 cm^{-1} interval. The difference between these two quantities decreases with wider lines and thus with increasing pressure; it also decreases with increasing average transmittance by the lines. We first assumed that $\ln \bar{T} = \ln \bar{T}'(\text{local}) + \ln \bar{T}'(\text{continuum})$ and that $(-1/u)\ln \bar{T}(\text{local}) = \bar{\kappa}(\text{local})$ in order to calculate $C^{o}_{s,p}$ and an approximate value of $\bar{\kappa}$(local) from data for two samples at different pressures. The approximate widths and spacings of the lines are known, so that by applying simple, band-model theory we were able to calculate a corrected $\bar{\kappa}$(local) and to adjust the values of $\bar{T}$, which were then used to determine a corrected value of $C^{o}_{s,p}$. In most cases, there was less than 10% difference between $(-1/u)\ln \bar{T}(\text{local})$ and $(-1/u)\overline{\ln T}(\text{local})$, so that the remaining error due to the averaging was probably not more than a few percent after the correction was made.

Average values of the quantities were calculated throughout the 1100 - 1500 cm^{-1} region for intervals 10 cm^{-1} wide, except near the points of inflection where narrower intervals were used. The results are presented in Fig. 3-4. The uncertainty in the plotted values of κ(local) and $C^{o}_{s,p}$ is greater in regions where one of the quantities is changing rapidly. For example, there is extra uncertainty in the heights and positions of the peaks of the upper curve near 1275 cm^{-1} and 1385 cm^{-1} where the lower curve is steep.

The general shape of the upper curve in Fig. 3-4 is similar to that expected for the $(100,0)_I$ and $(100,0)_{II}$ intrinsic bands of the 628 molecule. The P- and R-branches are evident, and the band centers agree well with the calculated values given in Table 3-1. Because of the relatively coarse spectral resolution used in the calculations, the line structure apparent in Fig. 3-1 has been smoothed. Any obvious contribution by the same bands of the 627 isotope or by the difference bands of the 626 isotope is obscured by the coarse resolution and the scatter in the experimental points. However, these bands undoubtedly contribute to the absorption in accordance with the discussion near the beginning of this section. The integrated absorption coefficient for the intrinsic absorption by the local lines expressed in $molecules^{-1}$ cm^2 cm^{-1} is 43.9×10^{-24} from 1200 to 1310 cm^{-1}, and 64.5×10^{-24} from 1310 to 1420 cm^{-1}. The estimated uncertainty is $\pm$ 10 percent.

The lower panel of Fig. 3-4 shows a spectral curve of the normalized absorption coefficient for pressure-induced absorption. The absorption peaks agree well with the calculated band centers 1285.43 and 1388.20 cm^{-1}, given in Table 3-1 for the pressure-induced bands of the 626 isotope. The absorption by the 627 and 628 molecules probably have a pressure-induced component, but it is apparently much smaller than that by the 626 molecule. The two bands are seen to overlap and to produce measurable absorption over a wider spectral interval than that covered by the intrinsic bands illustrated in the upper panel. Except near the peak at 1388 cm^{-1}, the data points corresponding to different samples agree within the expected experimental error. Below approximately 1130 cm^{-1}, the continuum is influenced by the wings of the lines centered from about 1000 cm^{-1} to 1100 cm^{-1}.

The integrals of the normalized coefficients in $molecules^{-1}$ cm^2 atm^{-1} cm^{-1} are 67.3×10^{-24} from 1130 to 1330 cm^{-1} and 101×10^{-24} from 1330 to 1500 cm^{-1}; the estimated uncertainties are $\pm$ 8 percent. We note that the ratio of the integrals is approximately 3 to 2, the same as that for the corresponding intrinsic bands.

Curves of κ(local) and C^{o}_{s} are shown in Fig. 3-5 for the region between 1490 and 1835 cm^{-1}. Since not all the continuum is due to pressure-induced absorption, we have omitted the subscript p from C^{o}_{s} in Fig. 3-5. The symbol C^{o}_{s} is written without a p or w, which denote pressure-induced or

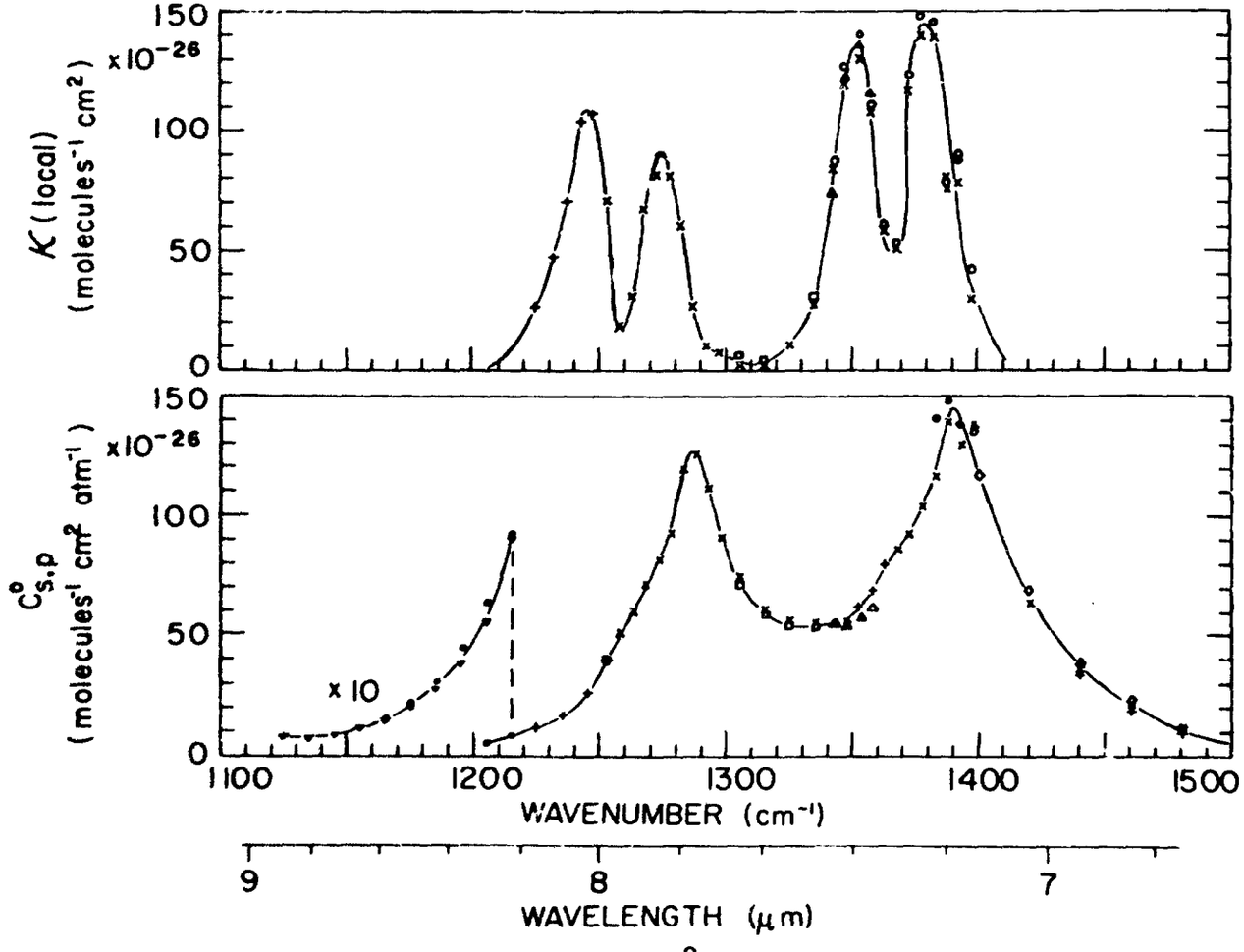

FIG. 3-4. Spectral Plots of κ(local) and $C^{o}_{s,p}$ for Pure CO_2 from 1100 to 1500 cm^{-1}. Values of $C^{o}_{s,p}$ were multiplied by 10 before they were plotted to form the short curve below approximately 1215 cm^{-1}.

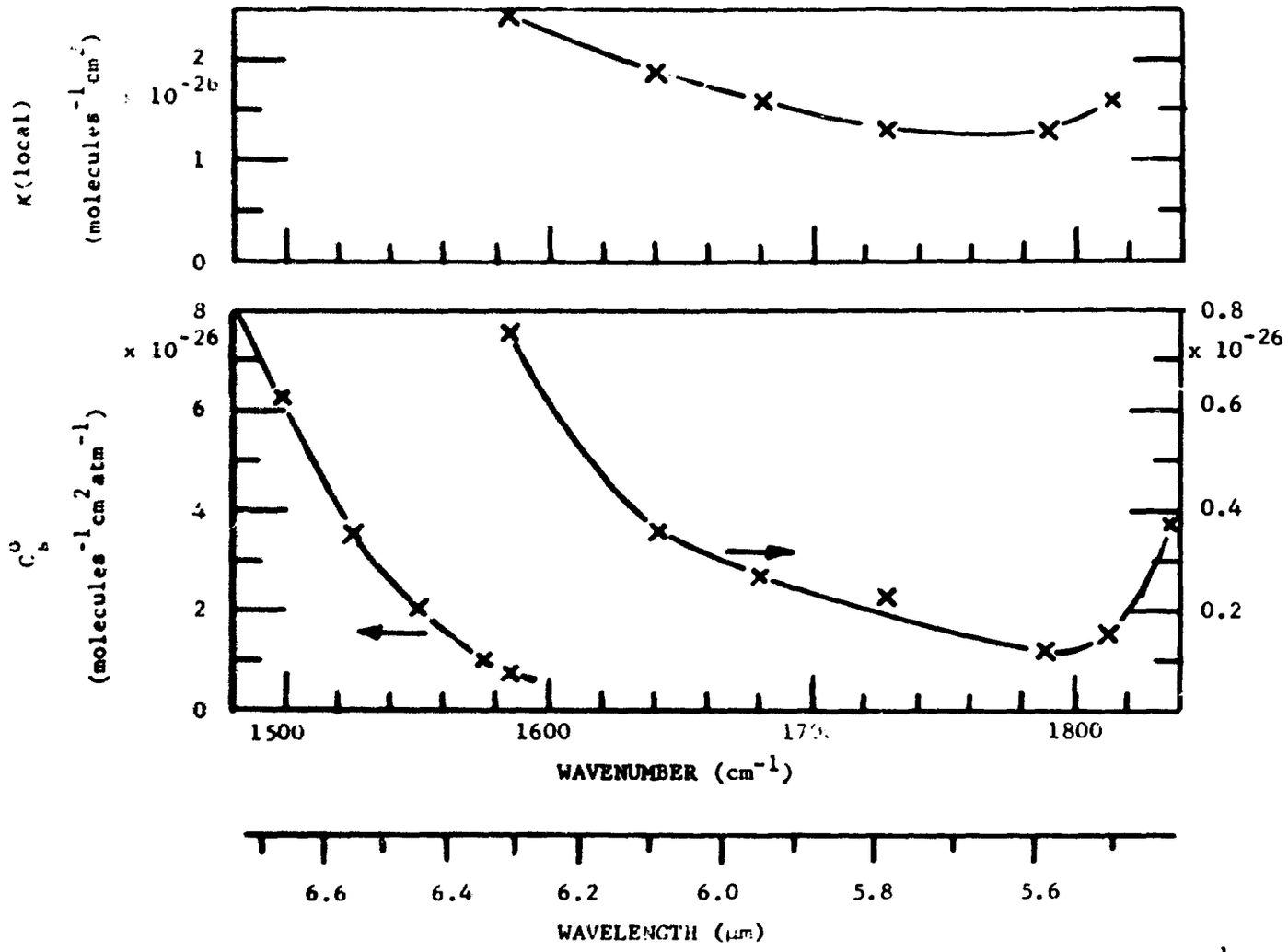

FIG. 3-5. Spectral Plot of κ(local) and C_s^c for Pure CO_2 from 1490 to 1835 cm^{-1}. The upper curve is subject to considerable error and probably represents maximum values. Each curve in the lower panel is read from the ordinate scale indicated by the arrow. Some of the continuum absorption, particularly from 1790 to 1835 cm^{-1}, probably results from the wings of lines centered at higher wavenumbers.

wing absorption, respectively, when the type of continuum is now known, or, in some cases, when it is clear which is being considered. The curve in the lower panel from 1490 to 1590 cm^{-1} is based primarily on Samples A and D whose transmittance curves are shown in Fig. 3-3. Samples B and C form the bases for the curves in Fig. 3-5 above 1585 cm^{-1}. The most serious errors between 1490 and 1850 cm^{-1} arise from absorption by the H_2O impurity. Near the H_2O band center at approximately 1585 cm^{-1}, the H_2O absorption is less than on either side. At this point the estimated error in C_s^o is between 0.1 and 0.2 x 10^{-26} $molecules^{-1}$ cm^2 atm^{-1}. At other points between 1490 and 1585 cm^{-1}, the errors may be twice this large.

Near 1788 cm^{-1} the H_2O absorption is still bothersome, but it is much less than at most places between there and 1585 cm^{-1}. The estimated absorptance by the H_2O impurity in Sample B was approximately 2 percent, while that by the CO_2 was 8 percent. We also attempted to account for the H_2O absorption in Samples B and C at three other points between 1788 and 1590 cm^{-1}. These points were chosen between H_2O lines where the H_2O absorption was less than at any other point within several cm^{-1}. The estimated correction for H_2O absorptance was less than 5 percent at these points for B, the 21.3 atm sample contained in the shorter absorption cell. The correction for H_2O absorptance was as much as 10 percent to 15 percent at these same points for Sample C. At 1788 cm^{-1} the estimated uncertainty in the plot of C_s^o is 0.05 x 10^{-26} $molecules^{-1}$ cm^2 atm^{-1}; at other wavenumbers between 1788 and 1585 cm^{-1} it may be double this amount.

The source of the intrinsic absorption coefficient, apparently due to local lines since it is independent of pressure, is not understood. At 1585 cm^{-1} we observed approximately 78.5 percent transmittance for Sample C and 67.8 percent transmittance for Sample B after accounting for the H_2O absorption. If we had observed the same transmittances for B and 89.3 percent for Sample C, we would have concluded that there was no intrinsic absorption. The difference 78.5 percent versus 89.3 percent is greater than our estimated error; therefore, we conclude that there is some intrinsic absorption. Spectral curves in this region show no structure other than that due to H_2O lines. If a very weak CO_2 band occurred in this region, we would expect to see some structure due to the vibration-rotation lines, although the amount of intrinsic absorption is small enough that we cannot rule out this possibility. The apparent intrinsic absorption may result from an impurity, other than H_2O, which has no line structure that would be observed with the spectral resolution used in obtaining the data. It is also possible, although difficult to believe, that errors in correcting for the H_2O absorption account for the apparent intrinsic absorption.

We feel that the upper curve in Fig. 3-5 represents maximum values for κ(local) due to intrinsic absorption by pure CO_2. The correct values may be much less if errors were introduced by impurities. Above

approximately 1780 cm^{-1}, the increase in κ(local) is due to very weak lines which are a part of the band seen near 1900 cm^{-1} in Fig. 3-3. Between 1585 and 1490 cm^{-1} the pressure-induced absorption is much greater than between 1585 and 1800 cm^{-1}; it is also enough greater than any intrinsic absorption that none of the latter was detected.

SECTION 4

ABSORPTION COEFFICIENTS AND INTEGRATED ABSORPTANCE FOR CO_2 BETWEEN 1885 cm^{-1} AND 2132 cm^{-1}

The spectral region from 1885 to 2132 cm^{-1} contains several CO_2 bands whose strengths have not been determined, although several of the band centers and line positions have been measured, or can be calculated accurately, from available data. (See Ref. 6 for spectral curves and a table of band centers.) The first part of this section deals with experimental data obtained primarily to determine the strengths of the bands and of single branches of some of the bands. Particular attention was given to the Q-branches. The samples contain CO_2 with He added in order to broaden the lines and remove much of the structure so that the observed transmittance T was approximately equal to the true transmittance T'. Helium, rather than N_2, was used as a broadening gas since it is difficult to obtain N_2 which does not contain enough CO impurity to absorb in this region. Furthermore, the extreme wings of He-broadened lines are weaker and thus produce less continuum absorption. Since the absorption coefficient varies over a wide range of values, different absorber thicknesses were used in the different narrow intervals in order to produce transmittances which could be measured accurately.

Throughout most of the region, $(-1/u)\ln T$ changes slowly with increasing pressure in the range of pressures used, and $(-1/u)\int \ln T d\nu$ is essentially independent of pressure if the integration is performed over an interval including several lines. This result implies that most of the absorption within the narrow interval is due to lines centered within the interval. In a few regions, $(-1/u)\int \ln T d\nu$ over a narrow interval increases significantly with increasing pressure. These regions occur where the absorption is very weak and a large fraction of it apparently is due to continuum absorption by the wings of stronger lines which are centered several line widths away from the points of observation. In these cases, $(-1/u)\int \ln T(\nu) d\nu$ does not truly represent the integral of the absorption coefficient of the lines centered in the interval. Examples of such regions are at the absorption minima near Q-branches, and particularly near 1945 cm^{-1}, 1990 cm^{-1} and from 2135 cm^{-1} to 2200 cm^{-1}.

The strong absorption feature near 2077 cm^{-1} can be recorded easily in atmospheric spectra obtained from an aircraft with the sun as a source. The spectral curves shown in Figs. 4-12 to 4-15 provide laboratory data on known samples at 297°K for comparison with field data. Table 4-2 provides the parameters of the samples and values of $\int A(\nu) d\nu$ over several narrow spectral intervals. In order to better simulate air, we added a mixture of 80% N_2 and 20% O_2 as a broadening gas.

TABLE 4-1

INTEGRATED ABSORPTION COEFFICIENTS FOR CO_2

Spectral Region (cm^{-1})	$-\frac{1}{u}\int T(\nu)d\nu$ (molecules^{-1}cm^{2}cm^{-1})	Sample Parameters[a]			
		p (atm)	P (atm)	u (molecules cm^{-2})	L (meters)
1885.0 - 1916.6	32.0 x 10^{-23}	0.334	14.6	272 x 10^{20}	32.9
1916.6 - 1919.4	5.67 "	0.334	14.6	272 "	32.9
1919.4 - 1930.0	9.04 "	1.00	9.98	205 "	8.26
1930.0 - 1936.6	16.1 "	1.00	9.98	205 "	8.26
1936.6 - 1940.6	0.585 "	1.00	9.98	205 "	8.26
1940.6 - 1944.0	0.503 x 10^{-23}	1.00	9.98	205 x 10^{20}	8.26
1944.0 - 2030.0	13.7 "	4.00	9.16	3320 "	32.9
2030.0 - 2073.4	299 "	0.334	14.6	68.2 "	8.26
2073.4 - 2081.4	195 "	0.101	9.98	20.7 "	8.26
2081.4 - 2091.0	21.3 "	0.334	14.6	68.2 "	8.26
2091.0 - 2095.8	22.1 x 10^{-23}	0.101	9.98	68.2 x 10^{20}	8.26
2095.8 - 2105.8	9.43 "	0.334	14.6	68.2 "	8.26
2105.8 - 2109.4	5.42 "	0.334	14.6	68.2 x 10^{20}	8.26
2109.4 - 2111.2	2.22 "	0.334	14.6	68.2 "	8.26
2111.2 - 2114.8	4.91 "	0.334	14.6	68.2 "	8.26
2114.8 - 2126.6	9.32 x 10^{-23}	0.334	14.6	68.2 x 10^{20}	8.26
2126.6 - 2131.8	11.6 "	0.334	14.6	68.2 "	8.26
2131.8 - 2191.7	30.6 "	4.00	9.16	3320 "	32.9

[a]Sample parameters refer to the samples that were used in determining the integrated absorption coefficient. The samples consist of p atm of CO_2 with helium added to produce total pressure P.

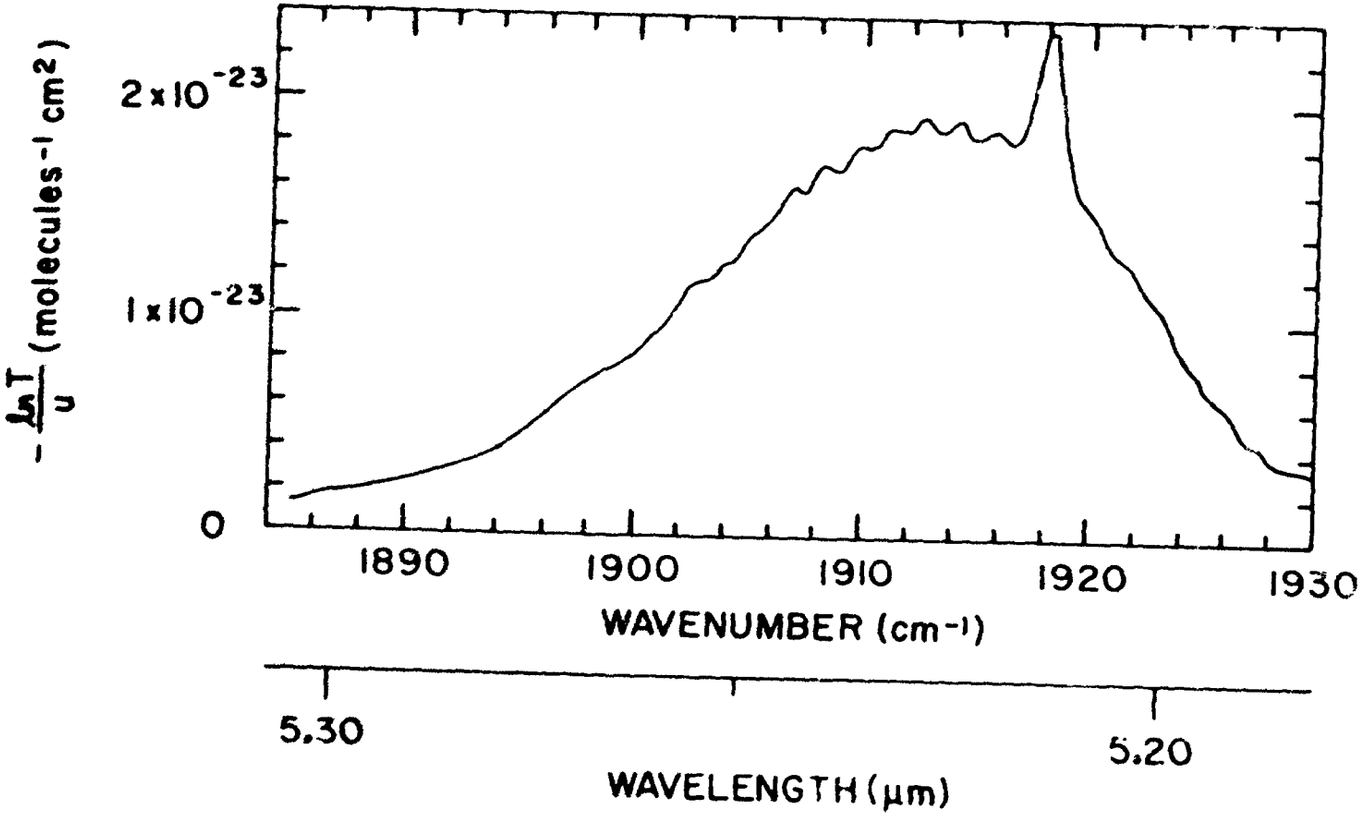

FIG. 4-1. Spectral Curve of $(-\ln T)/u$ for CO_2 from 1884 to 1930 cm^{-1}.

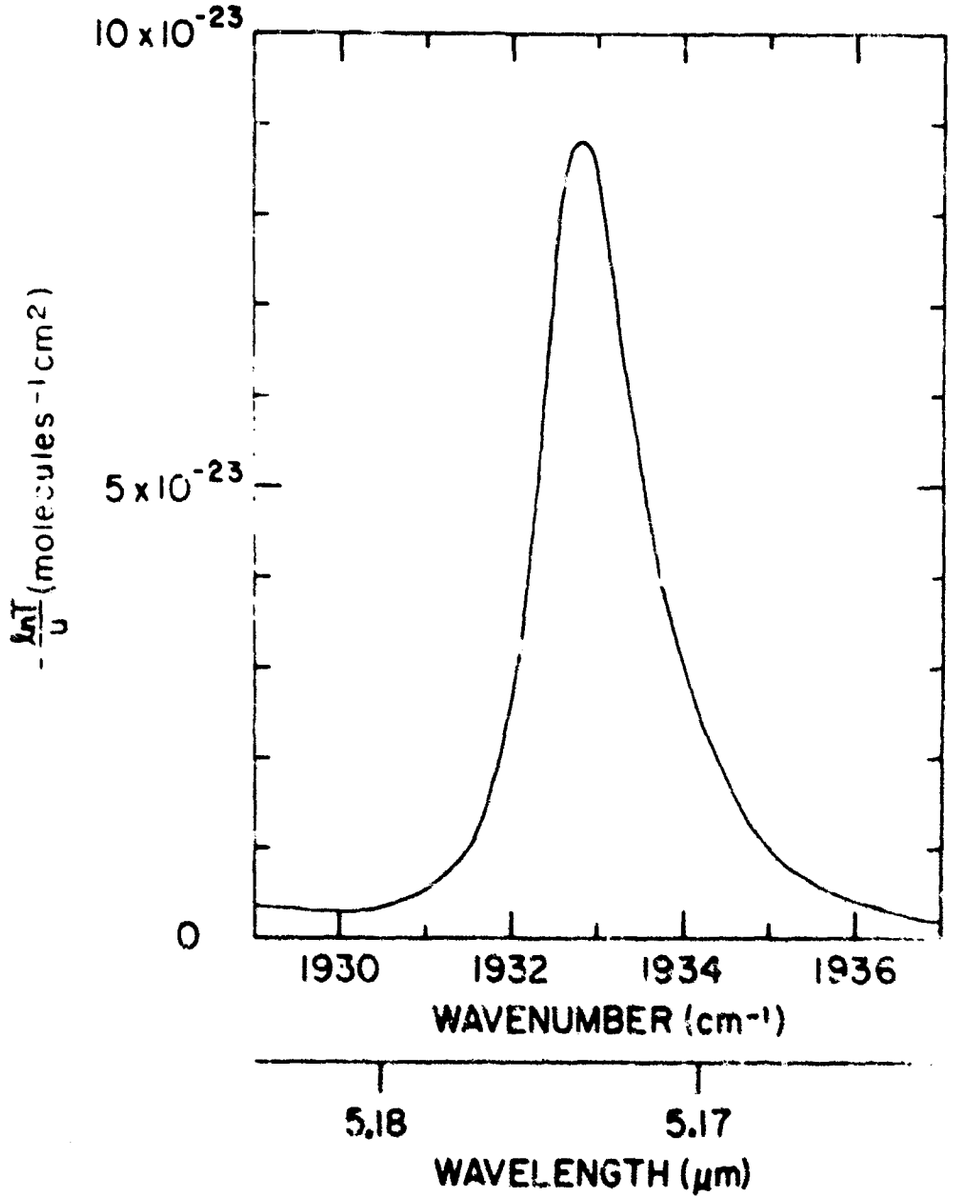

FIG. 4-2. Spectral Curve of $(-\mathcal{L}_{\nu}T)/u$ for CO_2 from 1929 to 1937 cm^{-1}.

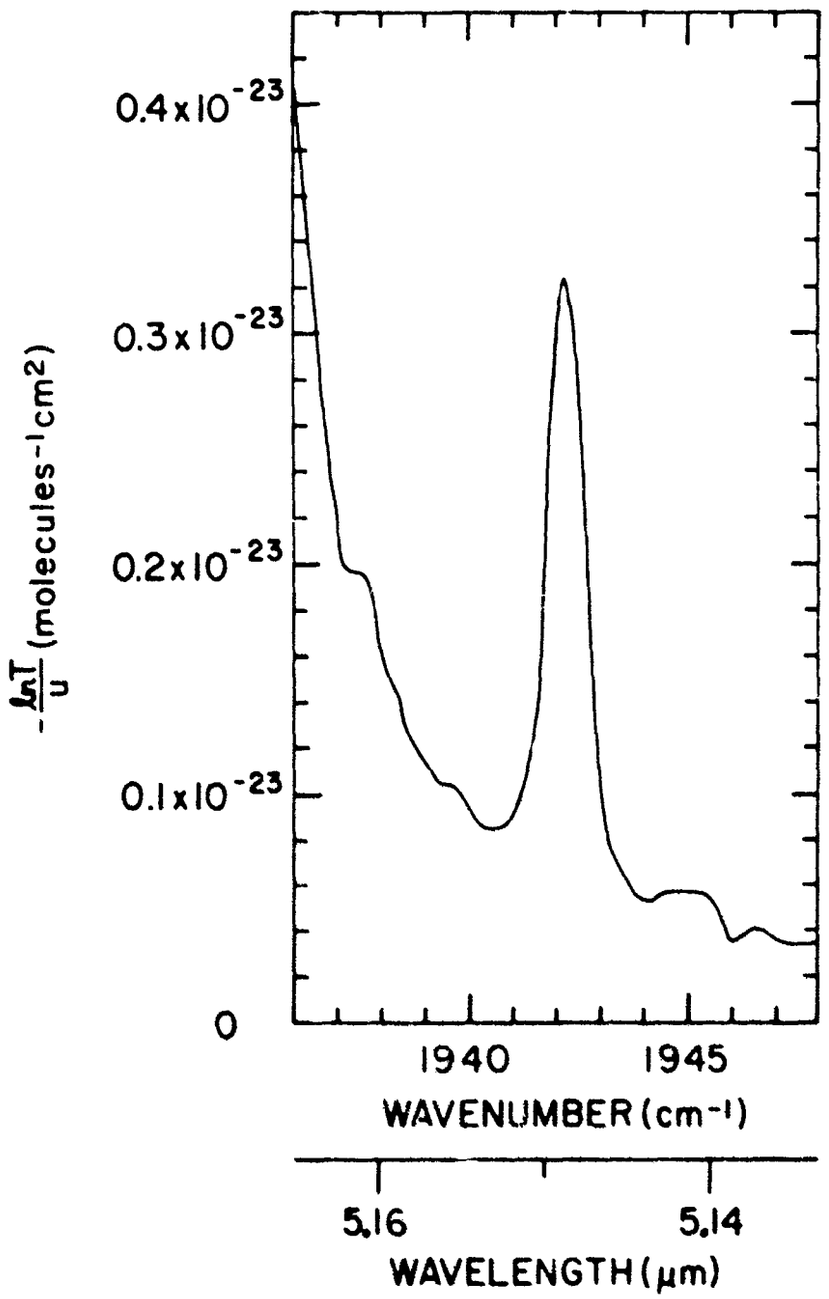

FIG. 4-3. Spectral Curve of $(-\ln T)/u$ for CO_2 from 1936 to 1948 cm^{-1}.

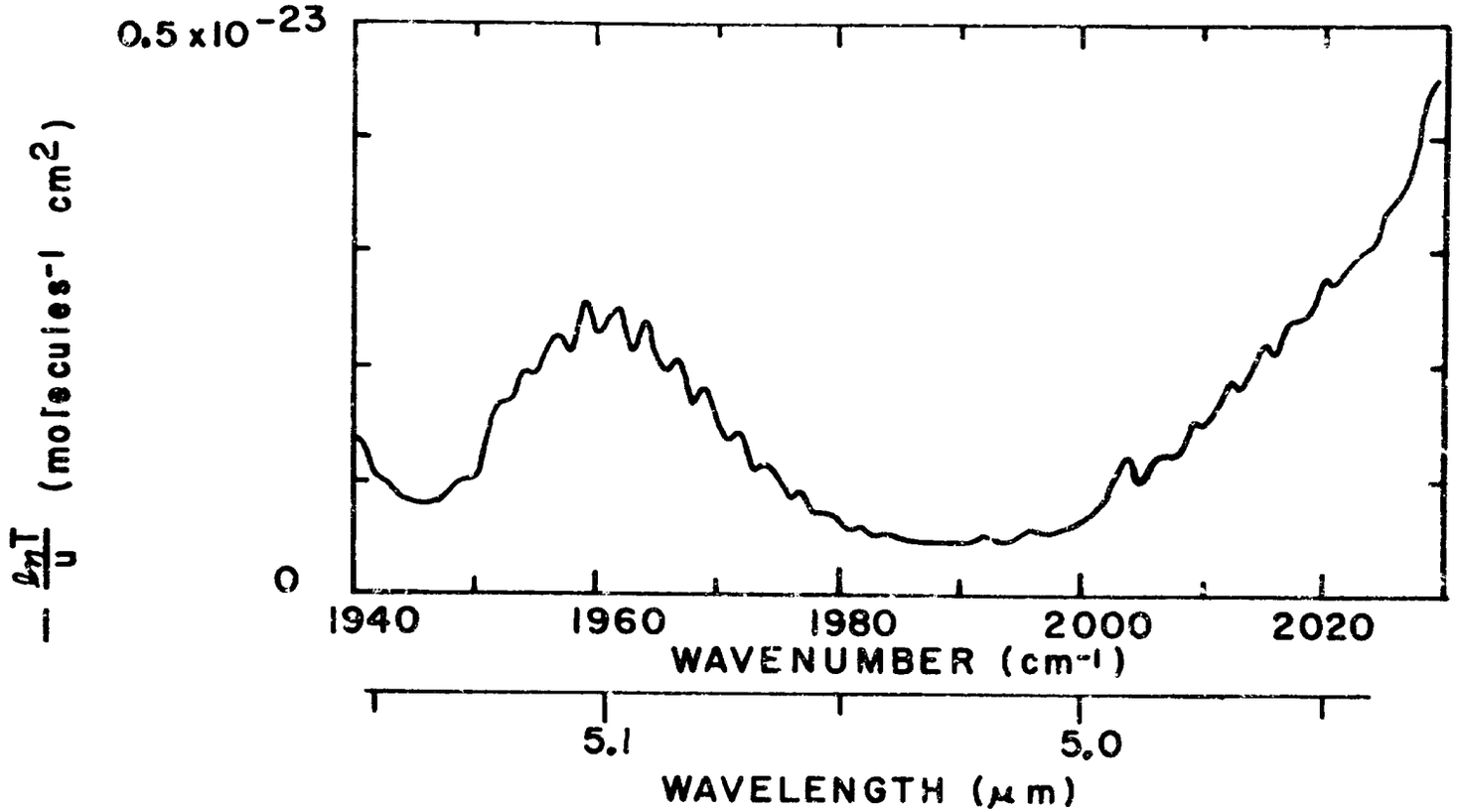

FIG. 4-4. Spectral Curve of $(-\ell nT)/u$ for CO_2 from 1940 to 2030 cm^{-1}.

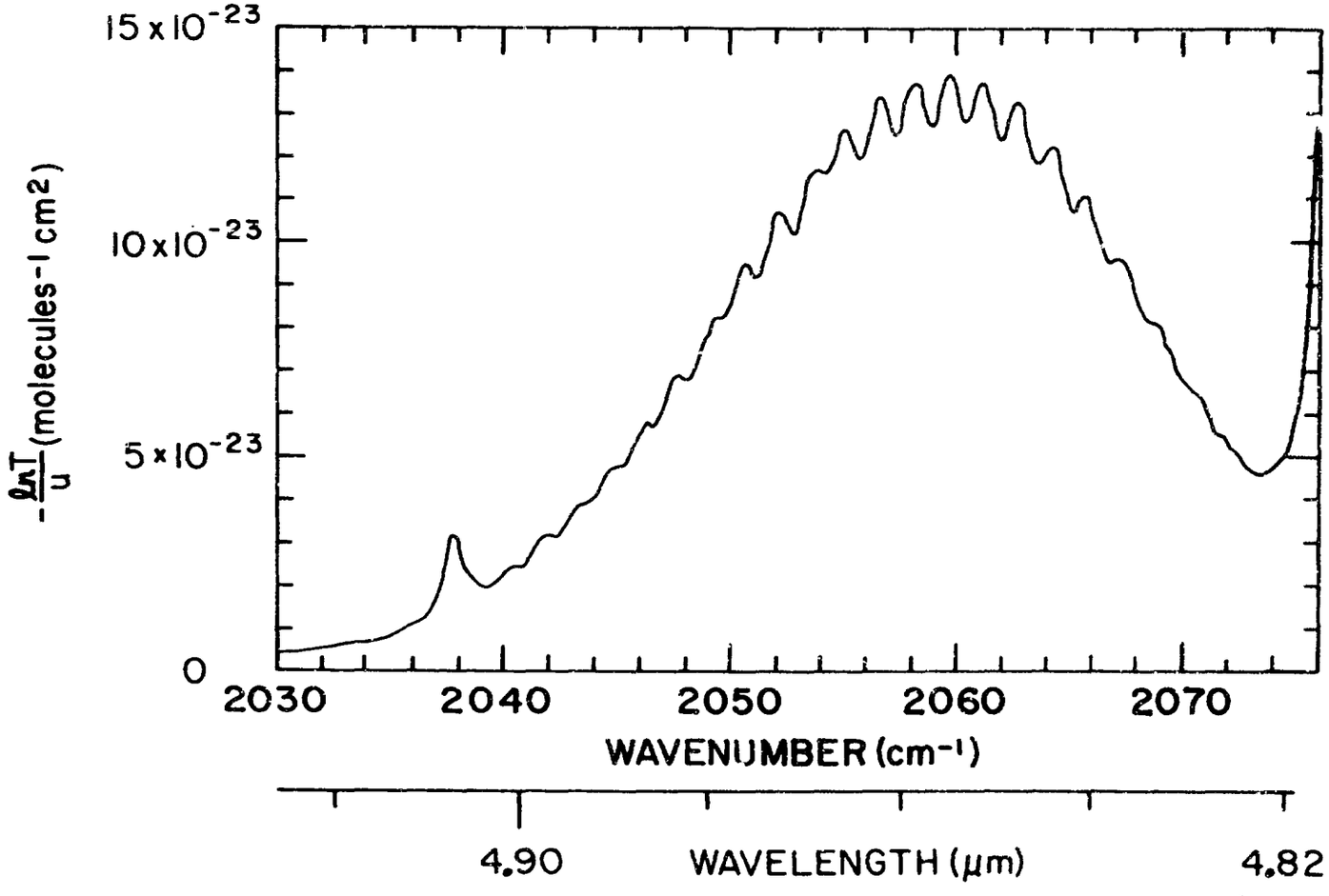

FIG. 4-5. Spectral Curve of $(-\ln T)/u$ for CO_2 from 2030 to 2076 cm^{-1}.

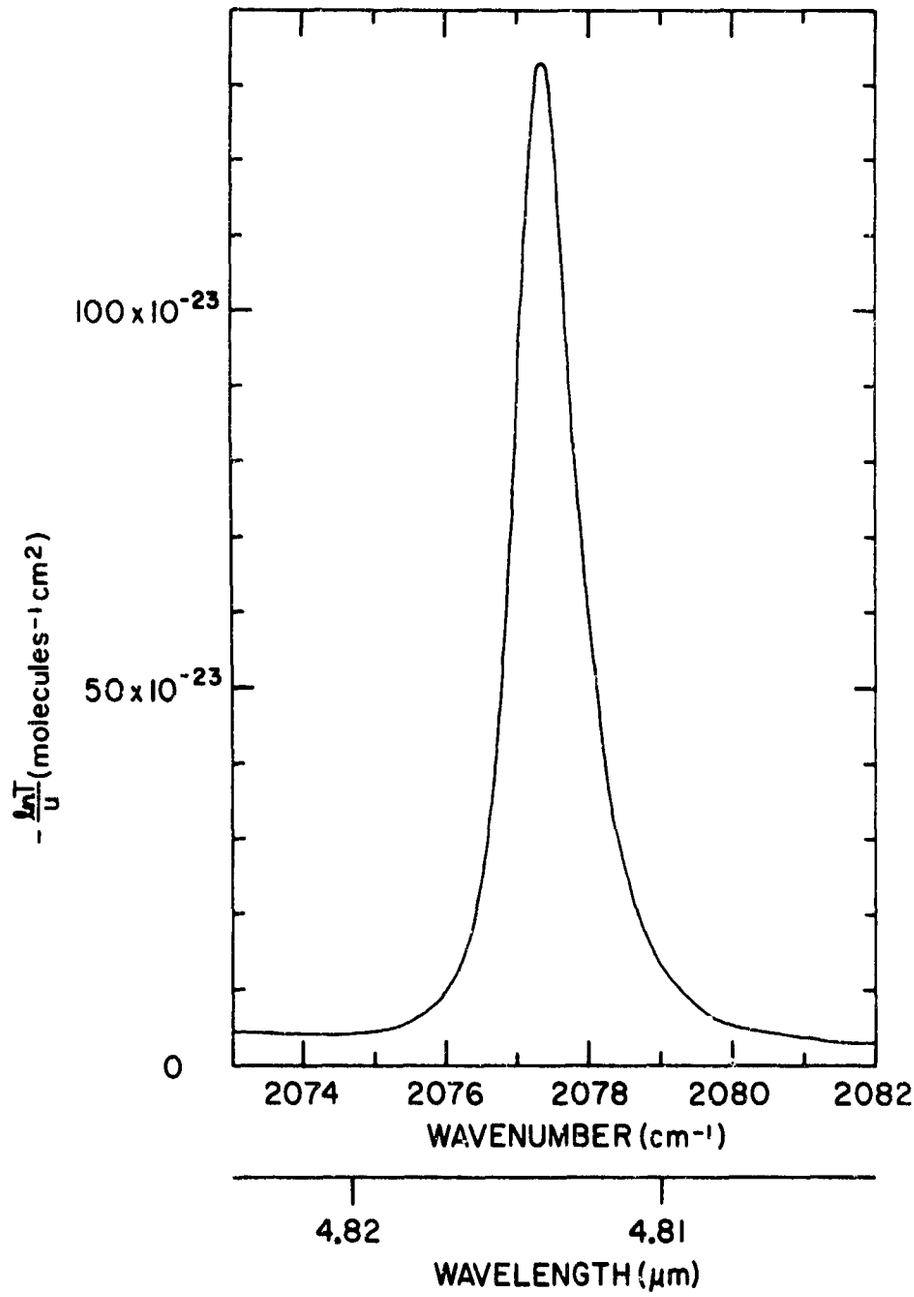

FIG. 4-6. Spectral Curve of $(-\ln T)/u$ for CO_2 from 2073 to 2082 cm^{-1}.

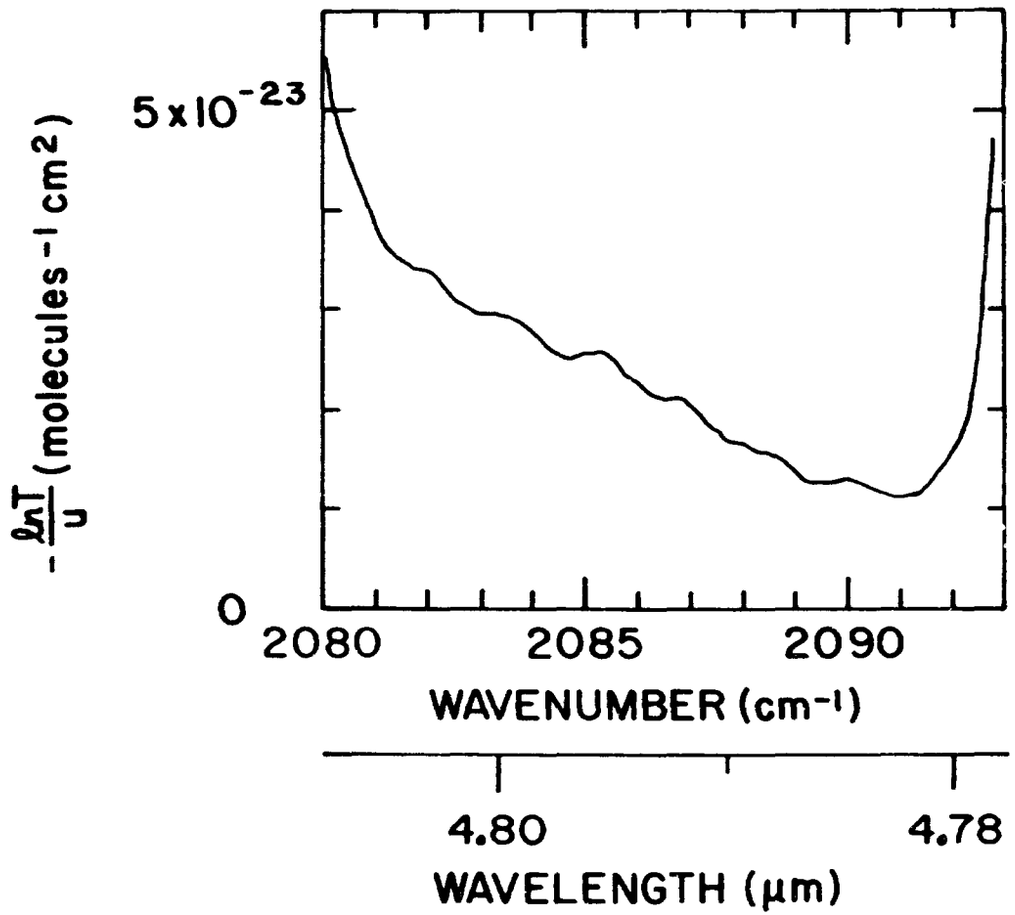

FIG. 4-7. Spectral Curve of $(-\ln T)/u$ for CO_2 from 2080 to 2093 cm^{-1}.

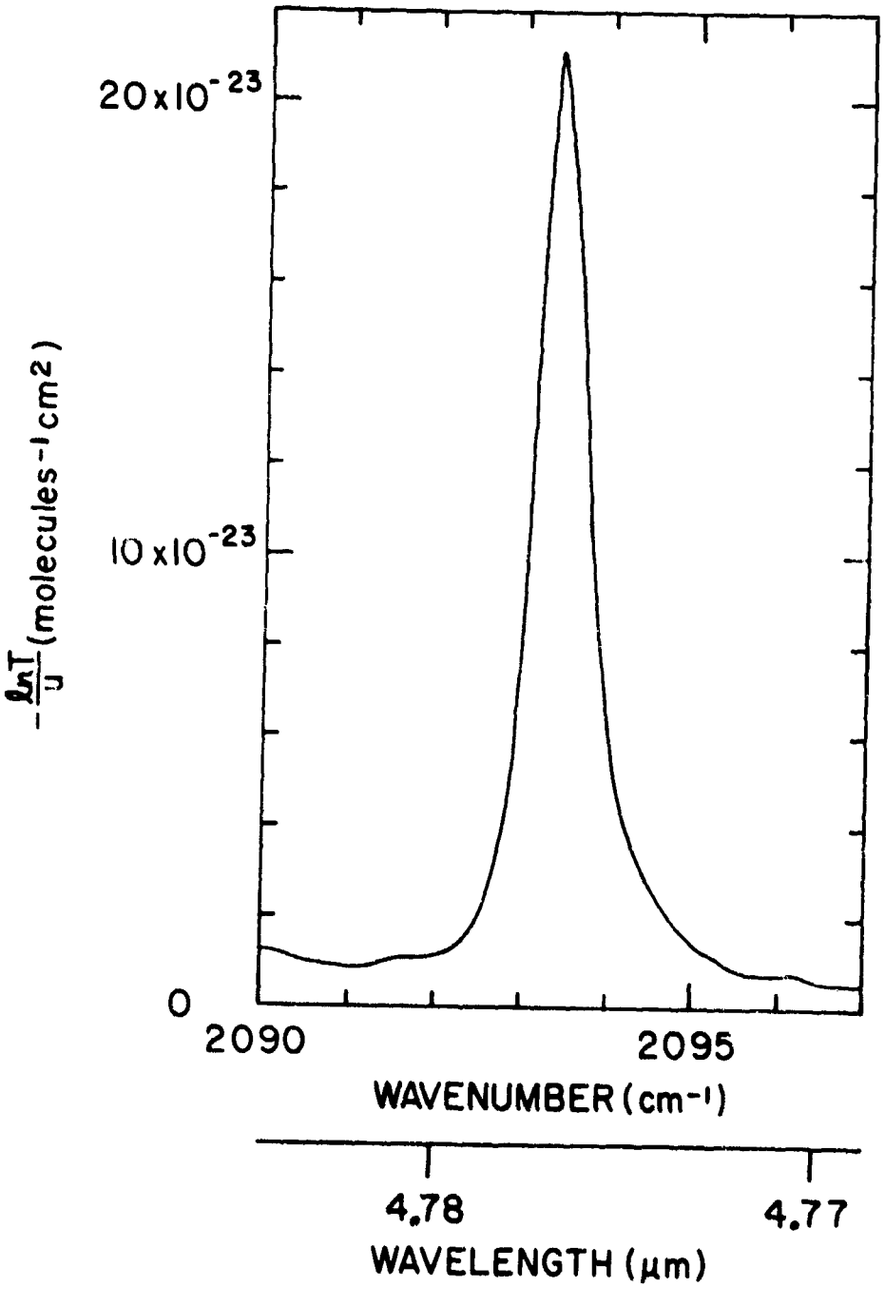

FIG. 4-8. Spectral Curve of $(-\ln T)/u$ for CO_2 from 2090 to 2097 cm^{-1}.

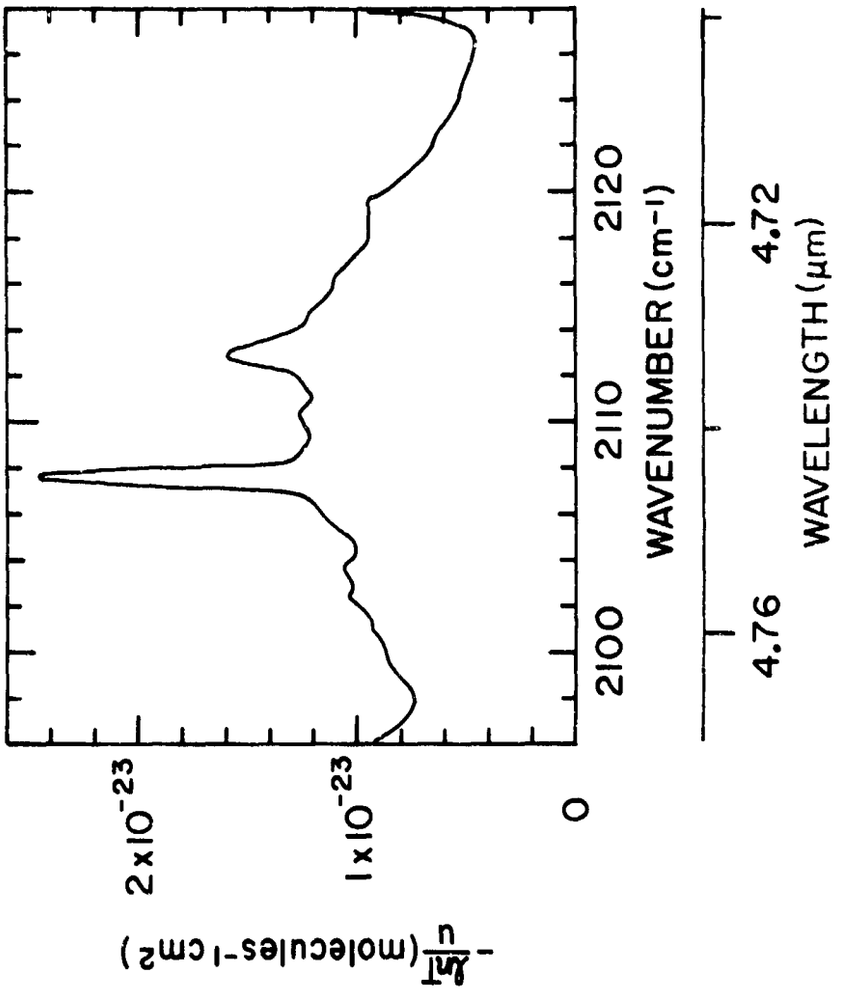

FIG. 4-9. Spectral Curve of $(-\Delta n_T T)/u$ for CO_2 from 2096 to 2128 cm^{-1}.

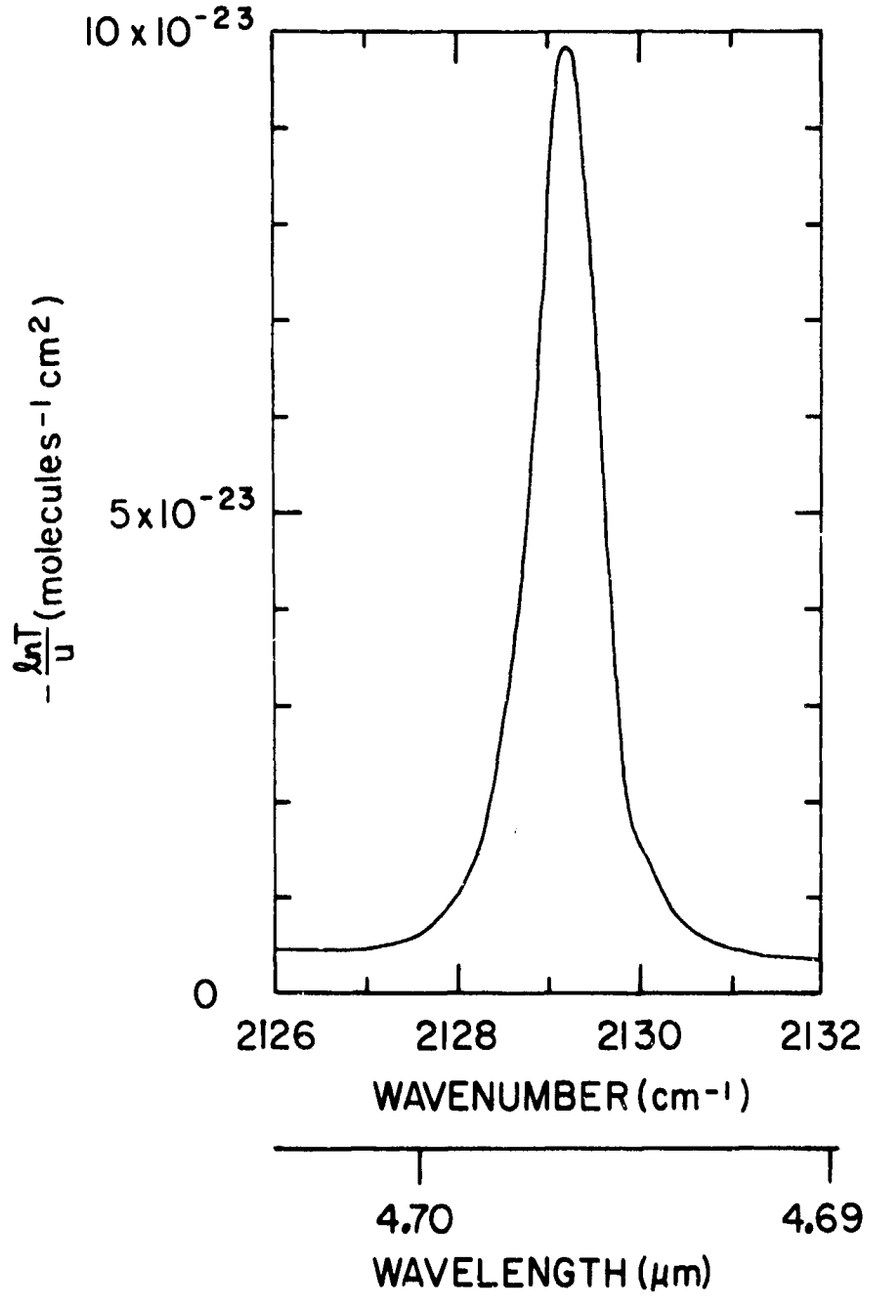

FIG. 4-10 Spectral Curve of $(-\ln T)/u$ for CO_2 from 2126 to 2132 cm^{-1}.

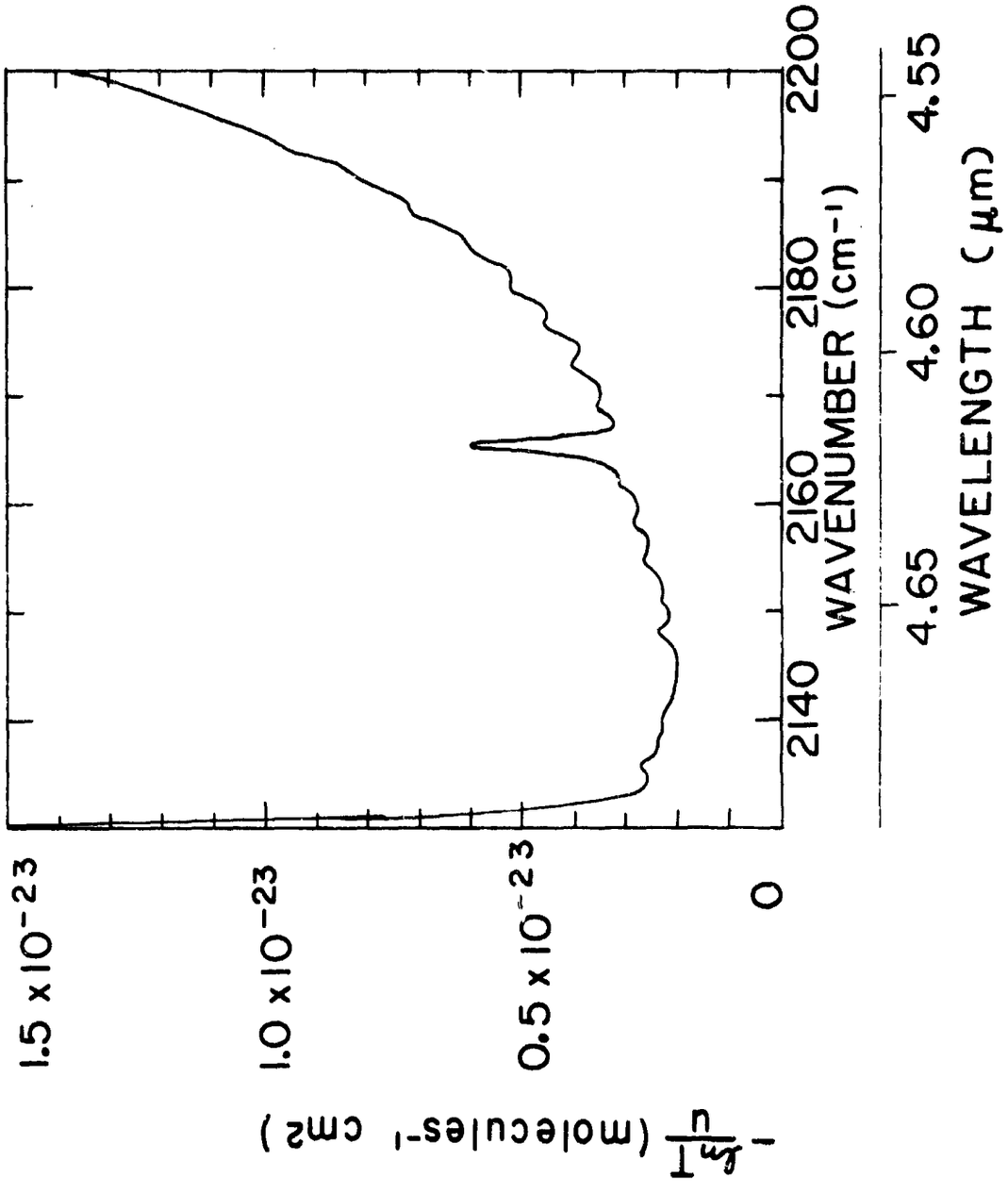

FIG. 4-11. Spectral Curve of $(-\ln T)/u$ for CO_2 from 2130 to 2200 cm^{-1}.

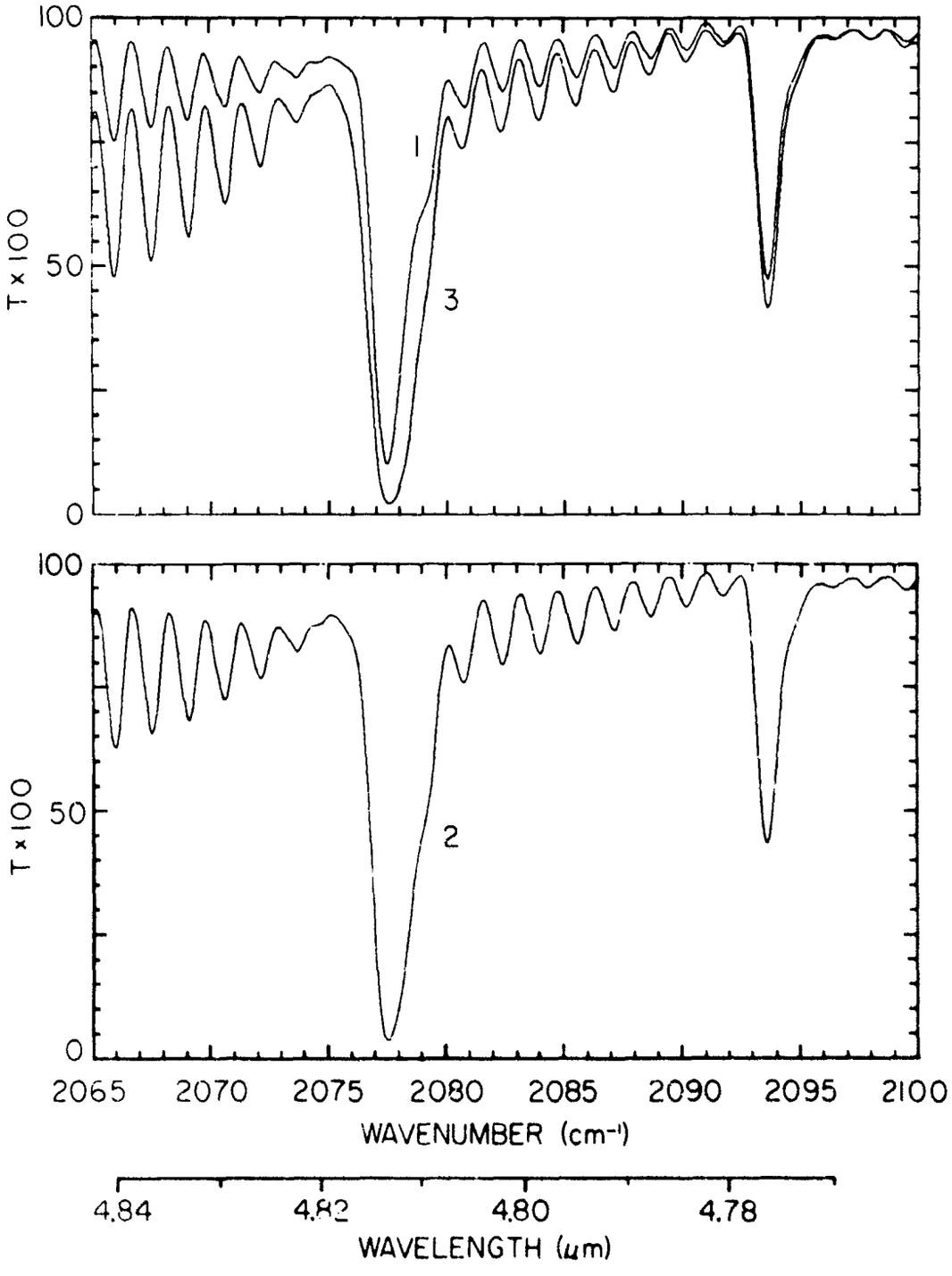

FIG. 4-12. Spectral Curves of Transmittance for CO_2 from 2065 to 2100 cm^{-1} for Samples 1, 2, and 3. See Table 4-2 for sample parameters and $\int A(\nu)d\nu$.

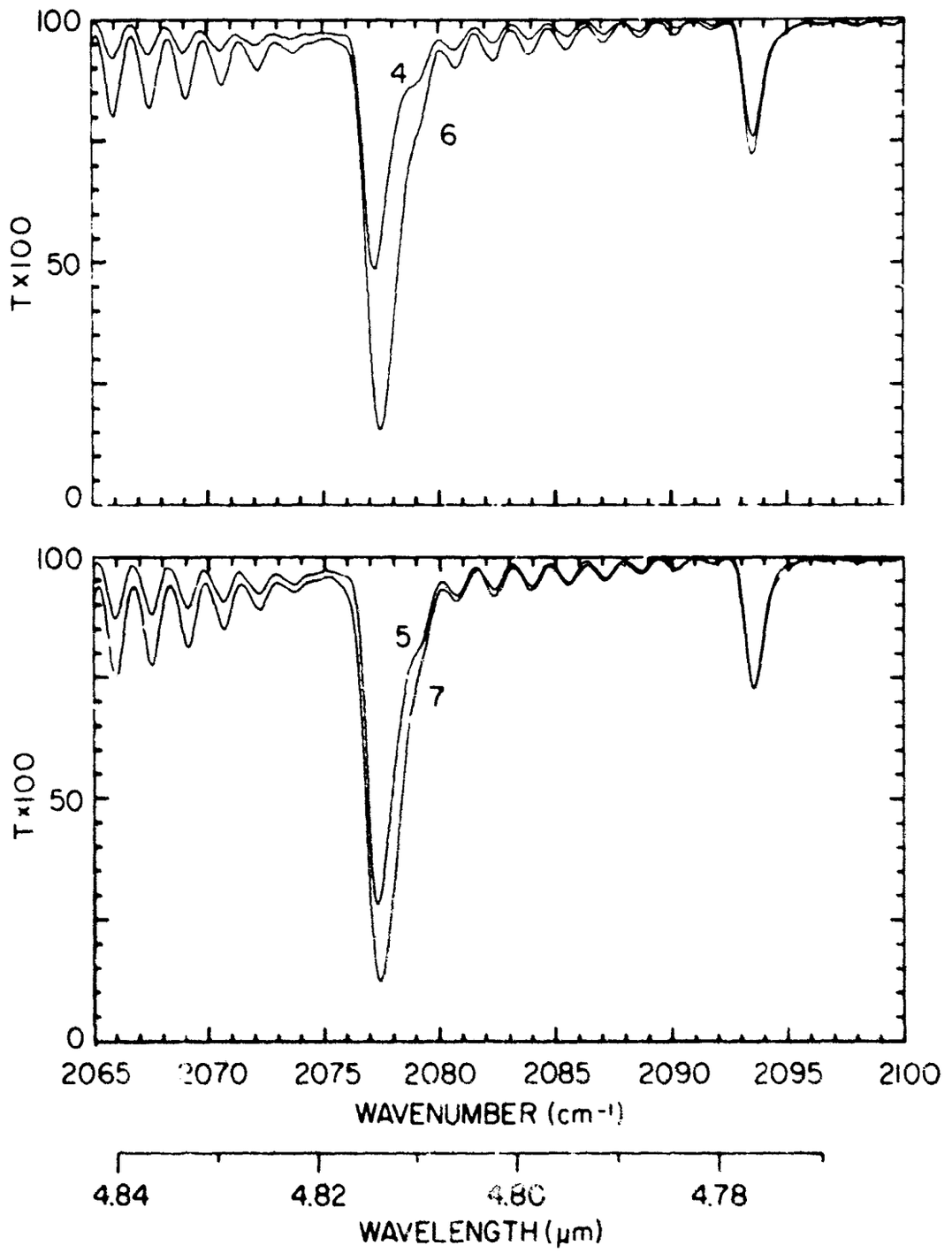

FIG. 4-13. Spectral Curves of Transmittance for CO_2 from 2065 to 2100 cm^{-1} for Samples 4, 5, 6, and 7.

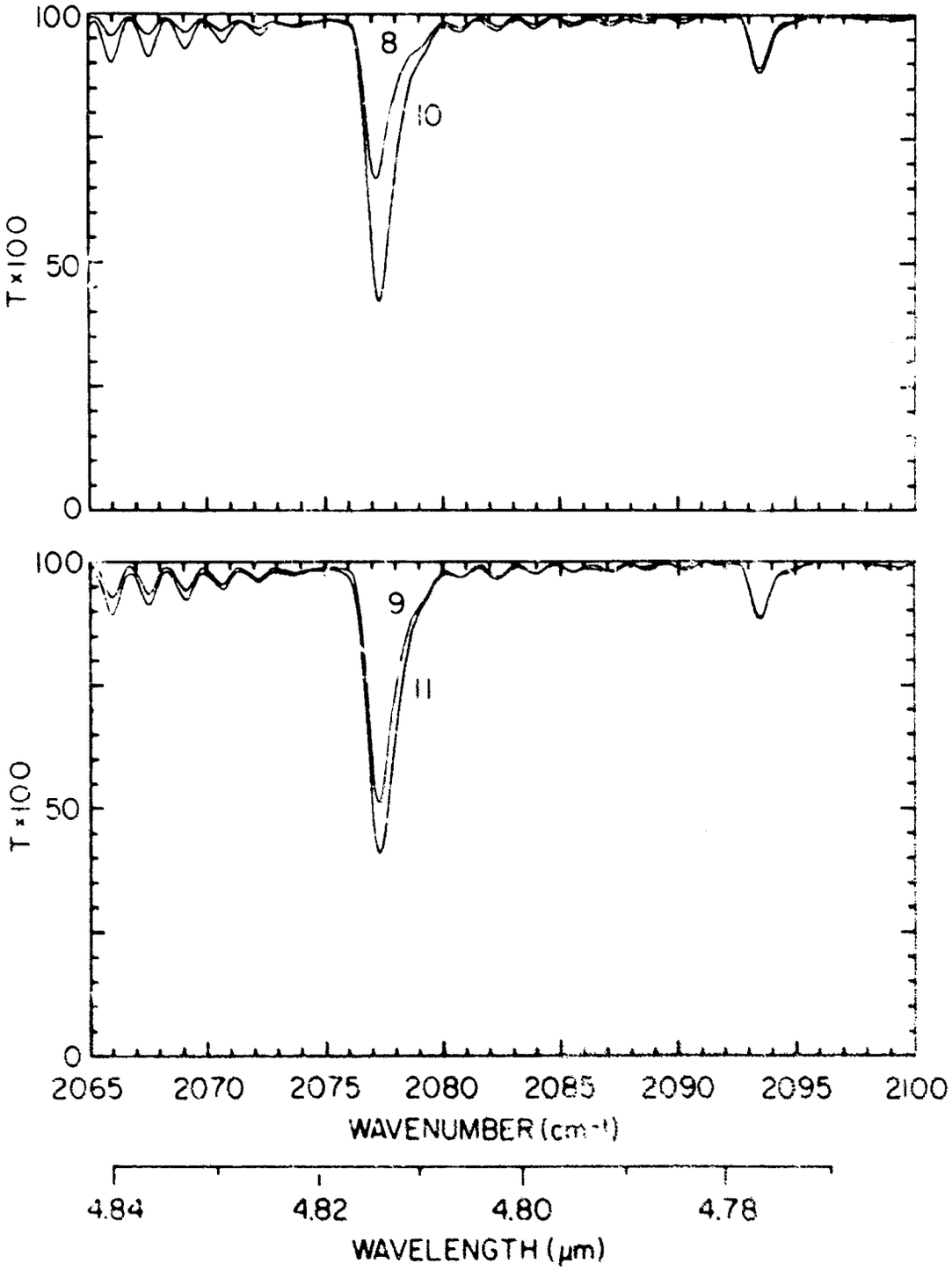

FIG. 4-14. Spectral Curves of Transmittance for CO_2 from 2065 to 2100 cm^{-1} for Samples 8, 9, 10, and 11.

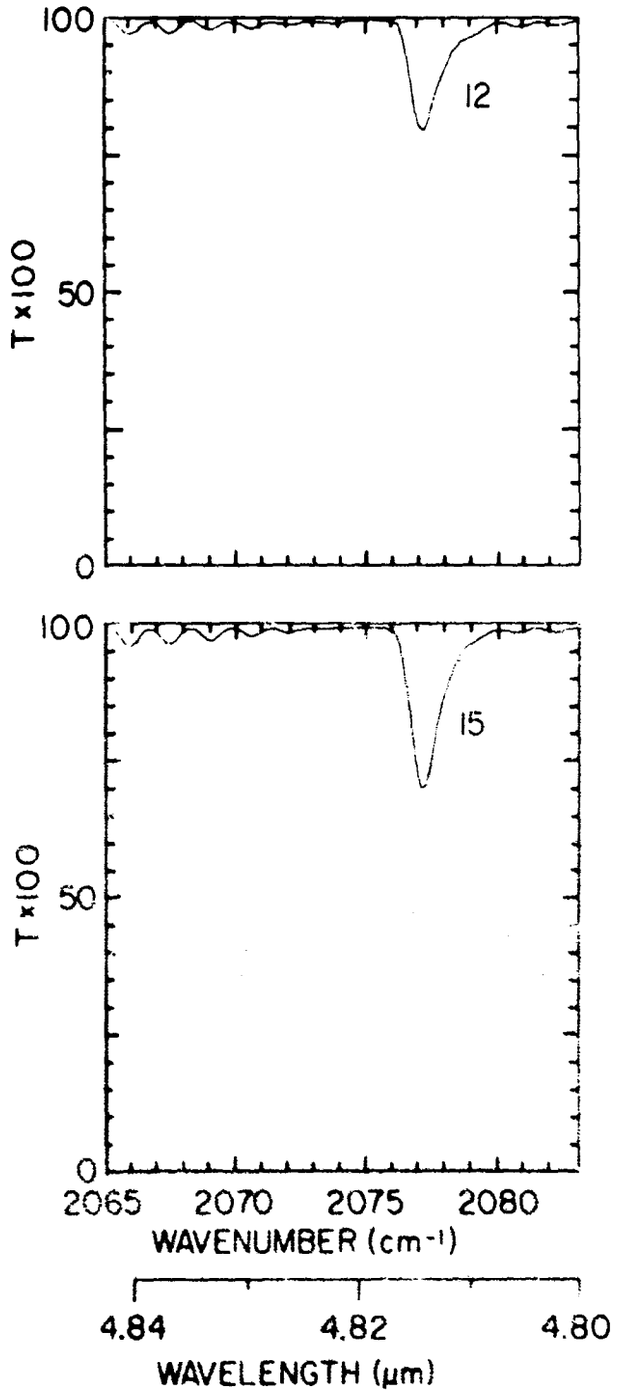

FIG. 4-15. Spectral Curves of Transmittance for CO_2 from 2065 to 2183 cm^{-1} for Samples 12 and 15.

Table 4-2

Sample Parameters and $\int_{\nu'}^{\nu} A(\nu)d\nu$

Sample No.	1	2	3	4	5	6	7	8	9	10	11	12	13	14	15
p(atm)	7.68 x 10^{-2}	7.68 x 10^{-2}	7.68 x 10^{-2}	2.32 x 10^{-2}	2.32 x 10^{-2}	2.32 x 10^{-2}	2.32 x 10^{-2}	8.03 x 10^{-3}	8.03 x 10^{-3}	8.03 x 10^{-3}	8.03 x 10^{-3}	8.03 x 10^{-3}	8.03 x 10^{-3}	8.03 x 10^{-3}	8.03 x 10^{-3}
L(meters)	32.9	32.9	32.9	32.9	32.9	32.9	32.9	32.9	32.9	32.9	32.9	32.9	32.9	32.9	32.9
u(molecules cm^{-2})	6.25 x 10^{21}	6.25 x 10^{21}	6.25 x 10^{21}	1.88 x 10^{21}	1.88 x 10^{21}	1.88 x 10^{21}	1.88 x 10^{21}	6.53 x 10^{20}	6.53 x 10^{20}	6.53 x 10^{20}	6.53 x 10^{20}	2.56 x 10^{20}	2.56 x 10^{20}	2.56 x 10^{20}	2.56 x 10^{20}
P Total(atm)	7.68 x 10^{-2}	2.79 x 10^{-1}	9.78 x 10^{-1}	2.32 x 10^{-2}	9.34 x 10^{-2}	2.93 x 10^{-1}	9.93 x 10^{-1}	2.76 x 10^{-2}	9.87 x 10^{-2}	2.92 x 10^{-1}	1.00 x 10^{0}	2.78 x 10^{-2}	9.67 x 10^{-2}	2.92 x 10^{-1}	1.00 x 10^{0}
P_a(atm)	1.02 x 10^{-1}	3.04 x 10^{-1}	1.00 x 10^{0}	3.08 x 10^{-2}	1.01 x 10^{-1}	3.01 x 10^{-1}	1.00 x 10^{0}	3.04 x 10^{-2}	1.01 x 10^{-1}	3.00 x 10^{-1}	1.00 x 10^{0}	3.04 x 10^{-2}	1.01 x 10^{-1}	3.00 x 10^{-1}	1.00 x 10^{0}
ν(cm^{-1})	$\int_{2065.2}^{\nu} cm^{-1}$	$\int_{2065.2}^{\nu} cm^{-1}$	$\int_{2065.2}^{\nu} cm^{-1}$	$\int_{2065.2}^{\nu} cm^{-1}$	$\int_{2065.2}^{\nu} cm^{-1}$	$\int_{2065.2}^{\nu} cm^{-1}$	$\int_{2065.2}^{\nu} cm^{-1}$	$\int_{2065.2}^{\nu} cm^{-1}$	$\int_{2065.2}^{\nu} cm^{-1}$	$\int_{2065.2}^{\nu} cm^{-1}$	$\int_{2065.2}^{\nu} cm^{-1}$	$\int_{2065.2}^{\nu} cm^{-1}$	$\int_{2065.2}^{\nu} cm^{-1}$	$\int_{2065.2}^{\nu} cm^{-1}$	$\int_{2065.2}^{\nu} cm^{-1}$
2065.20	0.	0.	0.	0.	0.	0.	0.	0.	0.	0.	0.	0.	0.	0.	0.
2066.70	0.219	0.344	0.532	0.094	0.106	0.171	0.233	0.037	0.059	0.091	0.096	0.028	0.033	0.038	0.041
2068.30	0.426	0.680	1.075	0.181	0.211	0.339	0.451	0.074	0.115	0.165	0.178	0.056	0.063	0.069	0.079
2069.80	0.628	0.996	1.516	0.267	0.309	0.491	0.656	0.109	0.167	0.237	0.250	0.078	0.087	0.096	0.110
2071.40	0.826	1.302	1.968	0.349	0.405	0.629	0.793	0.145	0.211	0.295	0.309	0.101	0.112	0.124	0.136
2073.00	1.011	1.581	2.385	0.425	0.493	0.746	0.922	0.179	0.248	0.338	0.356	0.118	0.135	0.152	0.159
2074.60	1.175	1.815	2.743	0.489	0.567	0.857	1.020	0.210	0.279	0.351	0.392	0.133	0.152	0.169	0.172
2076.10	1.307	2.001	3.044	0.543	0.630	0.946	1.101	0.230	0.300	0.378	0.424	0.143	0.166	0.182	0.186
2077.90	1.524	2.291	3.455	0.571	0.778	1.093	1.364	0.329	0.423	0.517	0.584	0.200	0.245	0.244	0.276
2080.00	1.214	4.363	5.465	1.300	1.877	2.477	2.819	0.757	1.066	1.276	1.365	0.457	0.569	0.601	0.634
2081.60	3.421	4.669	5.801	1.371	1.967	2.588	2.927	0.765	1.099	1.315	1.425	0.479	0.590	0.621	0.659
2083.10	3.567	4.867	6.046	1.417	2.034	2.676	3.009	0.809	1.129	1.349	1.463	0.496	0.607	0.637	0.674
2084.70	3.705	5.055	6.285	1.456	2.096	2.763	3.090	0.829	1.155	1.376	1.489				
2086.30	3.828	5.200	6.456	1.490	2.148	2.835	3.163	0.846	1.177	1.400	1.513				
2087.90	3.924	5.331	6.609	1.519	2.191	2.890	3.193	0.859	1.194	1.425	1.537				
2089.40	4.005	5.437	6.727	1.541	2.218	2.894	3.228	0.867	1.218	1.441	1.551				
2091.00	4.066	5.520	6.817	1.557	2.238	2.911	3.251	0.875	1.232	1.460	1.569				
2092.60	4.113	5.587	6.883	1.570	2.250	2.916	3.267	0.883	1.241	1.470	1.576				
2093.40	4.281	5.370	7.078	1.648	2.336	3.033	3.361	0.927	1.288	1.517	1.617				
2095.80	4.324	5.316	7.657	1.431	2.744	3.246	3.540	0.993	1.372	1.605	1.706				
2097.20	4.821	6.374	7.704	1.611	2.515	3.267	3.590	1.077	1.380	1.610	1.708				
2098.70	4.969	6.430	7.756	1.565	2.568	3.276	3.593	1.063	1.392	1.621	1.714				

SECTION 5

TRANSMITTANCE DATA STORED ON MAGNETIC TAPE

Under a previous contract, NOnr 3560(00), our laboratory published a series of reports dealing with the absorption of infrared radiation by CO_2 and H_2O. Each report is limited to a given spectral interval and contains detailed information on the absorption by several samples covering a wide range of pressures and path lengths. Tables of the integrated absorptance, $\int A(\nu)d\nu$, are included in all of this series of reports; some also include extensive tables of transmittance. As a result of requests from several workers in the field, we have compiled the transmittance tables on magnetic tapes which will be available through Air Force Cambridge Research Laboratories. The transmittance is tabulated versus wavenumber, and enough values are given so that the original spectral curves can be reconstructed without loss of structure by plotting the tabulated values and joining them with straight lines.

Table 5-1 summarizes the data saved on magnetic tape. The report number is the publication number assigned to the report by Aeronutronic. The absorbing gas and the spectral interval covered by the report are included in the table. A given file on the magnetic tape is devoted to the data from a single report.

TABLE 5-1

SUMMARY OF DATA SAVED ON MAGNETIC TAPE

Report Number	Absorbing Gas	Spectral Interval	
		cm^{-1}	μm
U-3704	H_2O	5,045 - 14,485	0.69 - 1.98
U-3202	H_2O	2,800 - 4,500	2.22 - 3.57
U-3200	CO_2	8,000 - 10,000	1.00 - 1.25
U-3930	CO_2	7,125 - 8,000	1.25 - 1.40
U-3127	CO_2	6,600 - 7,125	1.40 - 1.52
U-3201	CO_2	5,400 - 6,600	1.52 - 1.85
U-2955	CO_2	4,500 - 5,400	1.85 - 2.22
U-4132	CO_2	3,100 - 4,100	2.44 - 3.22
U-3857	CO_2	1,800 - 2,850	3.5 - 5.6

SECTION 6

REFERENCES

1. D. E. Burch, D. A. Gryvnak, and R. R. Patty, "Absorption of Infrared Radiation by CO_2 and H_2O. I. Experimental Techniques," J. Opt. Soc. Am. 57, 885 (1967).

2. D. E. Burch, D. A. Gryvnak, R. R. Patty, and Charlotte Bartky, The Shapes of Collision-Broadened CO_2 Absorption Lines, Aeronutronic Report U-3203, Contract NOnr 3560(00), 31 August 1968.

3. B. H. Winters, S. Silverman, and W. S. Benedict, J. Quant. Spectry Radiative Transfer 4, 527 (1964).

4. M. M. Shapiro and H. P. Gush, Canad. J. Phys. 44, 949 (1966).

5. C. B. Farmer and J. T. Houghton, Nature 209, pp 1341 and 5030 (1966).

6. D. A. Gryvnak, R. R. Patty, D. E. Burch, and E. E. Miller, Absorption by CO_2 Between 1800 and 2850 cm^{-1}, Aeronutronic Report U-3857, Contract NOn4 3560(00), 15 December 1966.

7. V. R. Stull, P. J. Wyatt, and G. N. Plass, The Infrared Absorption of Carbon Dioxide, Space Systems Div., Air Force Systems Command, Report SSD-TDR-62-127, Vol. III, Contract AF04(695)-96, 31 January 1963.

8. D. A. Gryvnak, D. E. Burch, Experimental Investigation of the Absorption by Various Gases of Planetary Interest, Aeronutronic Report U-4367, Contract 951712, JPL, 29 April 1968.

9. D. F. Eggers, Jr. and C. B. Arends, J. Chem. Phys. 27, 1405 (1957).

10. H. L. Welsh, M. F. Crawford, and J. L. Locke, Phys. Rev. 76, 580 (1949).

UNCLASSIFIED

Security Classification

DOCUMENT CONTROL DATA - R & D

Security classification of title, body of abstract and indexing annotation must be entered when the overall report is classified

1 ORIGINATING ACTIVITY (Corporate author)	2a. REPORT SECURITY CLASSIFICATION
Philco-Ford Corporation Aeronutronic Division Newport Beach, California 92663	Unclassified 2b GROUP

3 REPORT TITLE

INVESTIGATION OF THE ABSORPTION OF INFRARED RADIATION BY ATMOSPHERIC GASES

4 DESCRIPTIVE NOTES (*Type of report and inclusive dates*)

Scientific. Interim.

5 AUTHOR(S) (*First name, middle initial, last name*)

Darrell E. Burch
David A. Gryvnak
John D. Pembrook

6 REPORT DATE	7a. TOTAL NO. OF PAGES	7b NO. OF REFS
June 1970	50	10

8a CONTRACT OR GRANT NO	9a. ORIGINATOR'S REPORT NUMBER(S)
F19628-69-C-0263 ARPA Order No. 1366 b. PROJECT NO 5130 c DoD Element 62301D d DoD Subelement n/a	U-4829 Semi-Annual Technical Report No.1 9b. OTHER REPORT NO(S) (*Any other numbers that may be assigned this report*)

10 DISTRIBUTION STATEMENT

This document has been approved for public release and sale; its distribution is unlimited.

11 SUPPLEMENTARY NOTES	12 SPONSORING MILITARY ACTIVITY
This research was supported by the Advanced Research Projects Agency.	Air Force Cambridge Research Laboratories L. G. Hanscom Field (CRO) Bedford, Massachusetts 01730

13 ABSTRACT

From spectral transmittance curves of very large samples of CO_2 we have determined coefficients for intrinsic absorption and pressure-induced absorption from approximately 1130 cm^{-1} to 1835 cm^{-1}. Most of the pressure-induced absorption arises from the forbidden ν_1 and $2\nu_2$ bands of the $O^{16}C^{12}O^{18}$ molecule. Curves of the absorption coefficients for samples of CO_2 pressurized to approximately 10 atm, or more, with He are presented throughout most of the region from 1885 cm^{-1} to 2132 cm^{-1}. These curves and a table of the integrated absorption coefficient are adequate to determine the strengths of most of the bands of significance in this region. Spectral transmittance curves of CO_2 absorption between approximately 2065 cm^{-1} and 2100 cm^{-1} are presented for a variety of samples. Curves of the pressure-induced absorption by N_2 are presented for the 2400-2650 cm^{-1} region.

DD FORM 1 NOV 65 1473

UNCLASSIFIED

Security Classification

14 KEY WORDS	LINK A		LINK B		LINK C	
	ROLE	WT	ROLE	WT	ROLE	WT
N_2						
CO_2						
Continuum						
Absorption						
Atmospheric Transmission						
Pressure-Induced Absorption						